The Role of Epidermal Primary Cilia in Atopic Dermatitis and Psoriasis

A Doctoral Dissertation

Presented to Osaka University

2021

Defri Rizaldy

Content

Summary

Primary cilia, a tiny organelle structure, is recognized by its important role in cellular maintenance including cell proliferation and differentiation by regulating multiple signaling pathways. Recently, it has become clear that the severity of diseases such as polycystic kidney disease and various cancers have been correlated with primary cilia. With regard to skin inflammation, especially atopic dermatitis and psoriasis, keratinocyte development has been severely deregulated. The purpose of this study is to understand the role of primary cilia in keratinocytes in inflammation condition. It will help to deepen the knowledge regarding the pathophysiology of inflammatory skin disorder and lead to the novel therapy. By this awareness, I confirmed the increase in epidermal primary cilia distribution in atopic dermatitis and psoriasis skin compared to normal skin sample. Thereafter, observation in primary keratinocyte showed that stimulation using Th2 and Th17 cytokines increased primary cilia formation, but stimulation using Th1 cytokines did not increase ciliogenesis. Moreover, I introduced the downregulation of desmoglein-1, a keratinocyte differentiation protein in primary keratinocyte, after knockdown of (Intraflagellar Transport Protein 88) IFT88, an essential protein in primary cilia. Additionally, IFT88 showed be to associated with phosphorylation of JNK, a stress-related signaling pathway in primary keratinocyte. These results suggested that primary cilia have important role on modulating keratinocyte differentiation. These finding provide a novel perspective for characterizing the phenomena of skin inflammation that irregular ciliogenesis found in atopic dermatitis and psoriasis correspond with a decline in keratinocyte maturation and the generation of defects in the skin structure.

1. Introduction

The epidermal layer executes solid protection through its typical characteristics by forming permeability barricade, mechanical protection, and also innate immune system[1]. Covering extra-wide organ, immunovigilance in skin is built by multiple cells and molecular agents. Immune response has critical responsibility in establishing primary interface stability protecting vital organ from the environment. Excessive of immune response will lead to chronic inflammation and autoimmunity, whereas incompetent reaction towards stress and invasion risk to develop subsequent infection thus trigger malignancies[2]. Generally, human skin is constructed by two main components: the dermis and multilayered epidermis. The epidermis contains multiple native immune cells in stratum spinosum layer, particularly Langerhans Cell, Vγ9Vδ2 T cells subset, and resident memory T cells[3–5]. Recently, concept of inducible skin-associated lymphoid tissue has been proposed as a pinpoint clustering of antigent presenting cell activation which modulate contact dermatitis[3,6]. The activation of immune response leads to deprivation of skin barrier properties[7–10]. Reciprocally, a decrease in barrier properties potentiate the modulation of the local immune component in the skin[2,3]. The defect of barrier function is shown to emerge as a disturbance of keratinocyte homeostasis in balancing both of proliferation and differentiation[11]. Activation of the immune response in the epidermis is also found to be a substantial factor which affected keratinocyte biology, this constitution explains an inter-correlated relationship between skin protective function, immune cascade activation, and keratinocyte development supporting epidermal morphogenesis. Disruption one of these aspects lead to the initiation of an inflammation environment. The illustration of pathogenesis interplay is shown in Figure 1.1. Among various kinds of skin inflammation diseases, atopic dermatitis and psoriasis have emerged as two most common type of skin inflammation with wide prevalence in populations.

Atopic dermatitis is described as inflammatory eczematous lesions causing intense itch and emerges as one of the most common skin disorders found in up to a fifth of total population in developed countries[12]. The pathophysiological aspect of atopic dermatitis has dubious point whether it is triggered by inside-out (endogenic)[13] or outside-in (exogenous) motive[14]. Although the main driven factor of atopic dermatitis remains unclear, the pathophysiology is undoubtedly well defined, highlighting some important points: disruption of the epidermal barrier, cutaneous inflammation, and alteration of proliferation and differentiation of keratinocytes. Disruption of skin barrier function results from multiple causes including genetic mutation and environmental factors such the use of strong detergent and excessive scratch activity[15]. Loss of barrier function brings indirect impact of inflammatory T cell infiltration, which is modulated by skin homing signaling molecules. A series of signaling pathways continue to increase the number of lymphoid cells producing Th2 cytokine which are primarily found in lesional atopy[16]. In addition, hyperplasia is found to be a common phenotype in atopic dermatitis[17]. The upregulation of keratinocyte proliferation marker, Ki67, followed by a decrease in filaggrin expression as differentiation marker, is found among lesional and non-lesional atopic dermatitis[18–20]. Identical to atopic dermatitis, psoriasis is also mediated by immune response and genetically related skin inflammation manifestation[21]. The pathophysiology of psoriasis relies on the axis of IL-23 and Th17 activation[21]; thus, the vital role of IL-17A and IL-22 is highlighted in the disease progression[9,22,23]. Furthermore, psoriasis presents hyperplasia condition modulated by Th17 activation[24]. In an identical manner to atopic dermatitis, the skin barrier is compromised based on sensitization of immune response in psoriasis[25]. Both atopic dermatitis and psoriasis may not be grouped as life-threatening disease; however, the decreases in quality of life are shown to be the most substantial effects caused by this inflammation condition.

Several study has proposed a system or model mimicking both of atopic dermatitis and psoriasis conditions to facilitate deeper understanding of molecular interplay in skin inflammation[26–28]. Almost all of them exhibit a wide point of view regarding skin inflammation. Many models focus on the keratinocyte biological aspect, particularly the causal analysis of disruption in keratinocyte homeostasis. In the cellular level, the balancing act of keratinocyte proliferation and differentiation is related to multiple factors. A recent study showed the importance of primary cilia in guarding epidermal morphogenesis aspect[29].

Primary cilia are described as antenna-like structure protruding from basal body and have pivotal role in proliferation and differentiation[30]. Figure 1.2 shows the general structure of primary cilia. Primary cilia have vital a role in the homeostasis of the interfollicular epidermis, and one of the impacts of cilia loss is abnormal differentiation[31]. Part of cell proliferation regulator is ruled by ciliary proteins, includes intraflagellar transport (IFT) proteins, polycystins, hedgehog (Hh) and β-arrestins. Moreover, balance adjustment between cell proliferation and differentiation is also regulated by signaling through platelet-derived growth factor receptor α (PDGFRαα) and Wnt pathway[32], which are known to have impact on NFκB pathway by modulating IKK activity induced by IL-1β in murine chondrocyte cell line[33]. Furthermore, lipopolysaccharides reportedly induces neuronal inflammation modulated by primary cilia[34]. Our recent study showed the immunological role of dendritic cells primary cilia in skin disease[35]. However, to date, no study focuses on the behavior of epidermal cilia during an inflammation environment. As primary cilia clearly exhibit important role affected multiple cell activity including proliferation and differentiation, there is a high possibility of primary cilia on the alteration of keratinocyte character caused by stress condition from the activation of inflammation cascade in the skin. In this study, I evaluated the role of epidermal primary cilia in atopic dermatitis and psoriasis as the activity and functions of primary cilia in skin inflammation remains unclear.

2. Methods

2.1 Atopic dermatitis and Psoriasis vulgaris skin sample

Formalin-fixed paraffin-embedded atopic dermatitis and psoriasis vulgaris skin sections were obtained from patients following the ethical guidelines of Osaka University (Approval Number: 29-2-1) and Nagoya City University (Approval Number: 60-18-0003).

2.2 Cell culture

Neonatal normal human epidermal keratinocyte (NHEK) cells were purchased from Lonza. NHEK cells were cultured in KGM Gold (Lonza, Basel, Switzerland). Sub-confluent NHEK (P2-P4) were cultured on eight-chamber slides (ThermoFisher) and stimulated using various cytokines (IL-1β, tumor necrosis factor alpha [TNFα], interferon gamma [IFNγ], IL-4, IL-13, IL-31, IL-17A, and IL-22; PeproTech, NJ, USA) at 37^{o}C and 5 % CO_2 for 48 h. The culture of primary keratinocyte was approved by ethical guidelines of Osaka University (Approval Number: 29-2-1).

2.3 Immunohistology and immunocytology

Immunohistology of formalin-fixed paraffin-embedded skin

Slides were deparaffinized and antigen retrieval was performed using Tris-EDTA buffer at a pH of 9. Primary antibodies were diluted in blocking solution. Table 1 lists the primary antibodies used in immunohistology. After overnight incubation at 4^{o}C with the primary antibody, the slides were incubated with secondary antibodies containing Hoechst33342 (1:1000), goat anti-mouse Alexafluor-488 and goat anti-rabbit Alexafluor-594 (1:200 each)-conjugated IgG (ThermoFisher) at room temperature for 2 h. After a final wash, slides were mounted with Prolong Gold (ThermoFisher). Slides were observed and five random images along basal membrane were acquired at an objectives

magnification of 100X in each skin sample using an Olympus confocal microscope FV1200 (Olympus, Tokyo, Japan). Ciliated cells and total cell number, as well as cilia sizes, were counted and measured respectively using ImageJ software.[14]

Immunocytology for NHEK and HaCaT cells

Paraformaldehyde (4%, Fujifilm, Tokyo, Japan)-fixed slides were washed with phosphate-buffered saline (PBS) and blocked by incubation in 5% bovine serum albumin with 0.1% Triton X-100 (Millipore Sigma) in PBS for 30 min at room temperature. Primary antibody staining was performed by overnight incubation at 4^{o}C. Table 1 lists the primary antibodies used in immunocytology. After washing with PBST, the second antibody mixture (Hoechst33342 and goat anti-rabbit Alexafluor-594 [1:1000 each] conjugated to IgG, ThermoFisher) was applied for 2 h at room temperature. After washing in PBST, the slides were fixed using a Prolong Gold. Ciliated cells were analyzed as previously described.

2.4 RNA interference

IFT88-, ARL13B-, and KIF3A-targeted small interfering RNA (siRNA) (sequence listed in Table 2) was purchased from Life Technologies, CA, USA. Knockdown was performed for 6 h using Lipofectamin RNAiMax (ThermoFisher) based on the manufacturer's recommended protocol. Silencer Select Negative Control No. 2 (ThermoFisher) was used as the control. One day after knockdown was initiated, the culture medium was changed and the cells were stimulated using IL-13, IL-17A, and IL-22 (PeproTech).

2.5 RNA isolation and quantitative real-time polymerase chain reaction (PCR)

After NHEK was washed with DPBS (ThermoFisher), phenolic RNA extraction was performed using TRI Reagent (MRC, Tokyo, Japan). Precipitation and purification of

RNA were performed using isopropanol and 70% ethanol (Fujifilm). cDNA was synthesized using QuantiTect Reverse Transcription Kit (Qiagen, Venlo, The Netherlands). The PCR mixture was prepared by Thunderbird SYBR (Toyobo, Tokyo, Japan) and the primer pairs for IFT88, ARL13B, KIF3A, and 18s (sequence listed in Table 3) were obtained from FASMAC (Kanagawa, Japan). The fold relative expression was quantified, and statistical analysis was performed using Prism 7 (GraphPad Software, La Jolla, CA, USA).

2.6 Western blotting

Cold DPBS was used to wash NHEK cells before lysing them in a radioimmunoprecipitation assay buffer (Santa Cruz Biotechnology) contained protease and phosphatase inhibitors (cOmplete mini and PhosSTOP, Roche, Basel, Swiss). The proteins were mixed with sample buffer (Biorad, CA, USA) and heated before loading into wells of a sodium deodecyl sulfate-polyacrylamide gel (TGX, Biorad). After the gel electrophoresis was complete, the proteins were transferred onto polyvinylidene difluoride membranes using a semi-dry method (Trans-Blot Turbo, Biorad). The membranes were submerged in the primary antibody mixture that had been diluted with either 5 % bovine serum albumin in Tris-buffered saline (TBS) or 5 % skim milk in TBS overnight at 4^{o}C. The following primary antibodies were used: anti-IFT88 (ProteinTech, 13967-1-AP, 1:1500); anti-ARL13B (ProteinTech, 17711-1-AP, 1:2000); anti-KIF3A (Abcam, ab11259, 1:1500) anti-β actin (CST, MA, USA, 4970, 1:1000); anti-phosphorylated JNK (CST, 4668, 1:1000); anti-phosphorylated p38 (CST, 4511, 1:1000); and anti-DSG1 (Merck, Darmstadt, Germany, MABT118, 1:1000). After three washes with 0.1% Tween-20 (Millipore Sigma) in TBS (TBST), the membranes were incubated with secondary antibodies that had been conjugated to horseradish peroxidase (Biorad,

1:2000) and diluted in either 5% skim milk or 4% BlockAce (Ds Pharma, Tokyo, Japan) for 2 h at room temperature. After subsequent washes with TBST, the membranes were treated using ECL solution (GE Healthcare, IL, USA). Images were acquired using an Amersham Imager 600 (GE Healthcare). Band intensity was quantified using ImageJ and statistically analyzed using Prism 7.

2.7 Microarray experiment

NHEK were cultured in six-well plate and treated either using RNA interference of ARL13B, IFT88, or KIF3A; and incubated with or without IL-13 stimulation. After subsequent 48 h stimulation, total RNA was isolated using the RNeasy Mini Kit (Qiagen). cRNA synthesis, labeling, fragmentation, and hybridization were performed using the GeneChip™ 3' IVT PLUS Reagent Kit (ThermoFisher) accordance with the manuifacturing protocol. The comparative analysis of obtained data was performed using Transcriptome Analysis Console Software (Thermo Fisher).

2.8 Bioplex Immunoassay experiment

NHEK were cultured in a 12-well plate. RNA interference of IFT88 and cytokines stimulation was performed as previously described. After a subsequent 48 h stimulation using cytokines, protein purification, isolation, hybridization, and detection were performed using the provided reagent and protocol from Bio-plex Multiplex Immunoassay system (Biorad).

2.9 Statistical analysis

Statistical analysis was performed with GraphPad Prism, version 7.04. Quantification and measurements of the percentage of ciliated cells and cilia length were compared between normal skin samples and atopic dermatitis or psoriasis skin samples using Mann-Whitney U tests. One-way analysis of variance, followed by Bonferroni’s post hoc test was used

to compare the percentage of ciliated cells after the stimulation of keratinocytes using multiple cytokines. The same statistical method was also used for western blot semi-quantitative analysis.

3. Results

To understand the role of epidermal cilia in skin inflammation diseases, first I analyzed the existence of ciliated cells in diseased skin and explored the plausible association with some protein expressions in the skin sample. Skin samples were provided by our research collaborator from Nagoya City University. A total of eight samples, obtained from different donors, of normal skin, fifteen samples of atopic dermatitis skin, and eight samples of psoriasis skin were used in this analysis. The research was followed by a functional analysis study of primary cilia using normal human epidermal keratinocyte (NHEK) to seek the possibility of primary cilia function under inflammation conditions.

3.1 Observation of ciliated cell in the epidermis of normal, atopic dermatitis, and psoriasis skin samples

On the initial examination of primary cilia in the skin sample, I used anti-acetylated tubulin (AcTub) antibody as the primary cilia marker. Previous study of primary cilia also used anti-AcTub to dye the ciliary shape in human skin sample[36]. Fluorescent immunohistochemistry (IHC) of normal, atopic dermatitis, and psoriasis skin samples revealed a green ciliary structure in the blue signal of Hoechst 33342 (Fig. 1, 2, and 3). However, some non-specific signals were also shown as background in green color. This result is understandable as tubulin, which is a major component comprising cell structure and shape. From these results, ciliated cell was found in higher number in atopic dermatitis and psoriasis skin sample compared with normal skin sample as pointed by white arrowheads in Figures 1, 2, and 3. Multiple options are available for primary cilia staining. To mark the axoneme structure of primary cilia, some intraflagellar (IFT) protein marker can be utilize to describe the presence of primary cilia, in example IFT88 and

IFT20. Moreover, a group of GTPase which localized in cilia, such as Adenosine diphosphate ribosylation factor-like protein 13B (ARL13B), has been commonly used for primary cilia staining[37].

In order to have proper visualization of primary cilia structure, I performed subsequent IHC of normal and diseased skin samples using double staining with a marker for basal body region of primary cilia, anti-pericentrin (PCT), shown in red color, and anti-ARL13B shown in green color based on a previous study[38,39]. The expression of ARL13B is enriched in the axoneme part of primary cilia. Figures 4, 5, and 6 show the costaining images of normal, atopic dermatitis, and psoriasis skin samples using a combination of primary cilia markers, respectively. Pericentrin is a substantial part of the centrosome, in which the initiation of ciliary shaft development is started. IHC staining of normal and diseased skin samples showed clear primary cilia structure over the skin sample. Not only in the epidermis area, but primary cilia were also found in the dermal area, which mainly consists of fibroblast cell in normal skin, shown under the white dash line (not pointed by white arrowhead) especially in atopic dermatitis and psoriasis skin samples (Figure 5 upper left panel and Figure 6 upper and lower right panel). The white dash line showed the basal membrane, which separated the epidermis and dermis structure. The magnification image, located in the lower panel in each figure, shows the pinpoint of each ciliary shaft (green) with centrosome (red). Similar to previous result, the general examination showed higher number of ciliated cell was found in atopic and psoriasis skin compare to normal skin.

3.2 Anatomical and statistical analysis of ciliated cells in the epidermis of normal, atopic dermatitis, and psoriasis skin samples

To confirm the gain of ciliated cell frequency, I counted the number of primary cilia found in particular position of each skin sample. Figure 4-6 shows that primary cilia are generally located around the basal membrane. This outcome proposed that ciliated cells are distributed along the basal layer of epidermis. To prove these hypothesis, normal, atopic dermatitis, and psoriasis skin samples were stained using an epidermal basal cell marker. Anti-cytokeratin 5 (K5) and anti-cytokeratin 14 (K14) were common biochemical makers for stratified epithelia, which includes the basal cell layer in the epidermis. Figure 7 shows the co-staining images of skin samples using anti-K14 antibody and anti-ARL13B antibody. In normal skin on the left panel, the expression of K14, revealed in red color, was strictly found along the basal layer, which is located close to the white dash line showing the border of the dermis and epidermis part of the skin. However, atopic dermatitis and psoriasis skin samples showed contrasting outcomes. The expression of K14 was not only confined to the cell in the basal layer but also in the keratinocytes on the suprabasal area. Spinous cells of atopic dermatitis and psoriasis skin also expressed K14 in comparable manner to the basal area as shown in magnified images on the lower panel of Figure 7. The expression of K14 indicates that keratinocytes are undifferentiated and commonly found in the basal layer of normal skin, as shown in the left panel of Figure 7. This outcome may explain the hypothesis of disturbance in keratinocyte differentiation found in skin inflammation. A similar issue is shown by previous studies regarding K14 expression pattern both in atopic dermatitis and psoriasis[22,35].

Next, I opted to use another biochemical marker of the basal cell layer. Besides K14, K15 displays identical expression in the basal layer of epidermis. Moreover, K15 has shown specific properties found in stem cell[40]. Figure 8 shows the double staining images of the

skin sample using anti-K15 antibody (red) and anti-ARL13B antibody (green). On the normal skin image on the left panel (upper part, and magnified images in the lower part), the red signal perfectly showed K15 expression on the basal cell layer, in which cells attached to the basal membrane in the epidermis. Comparably, K15 expression in atopic dermatitis and psoriasis skin also showed the localization near the basal membrane. However, particularly in atopic dermatitis skin, one or two layers around basal membrane still expressed K15. These phenomena may describe the hyper-proliferative activity of the epidermis resulted in hyperplasia which commonly develops in skin inflammation. Most of ARL13B shown in green signal was found in K15 positive cells on atopic dermatitis and psoriasis skin sample. However, one primary cilium (pointed by a red arrowhead in psoriasis-magnified image, right panel lower part) was located in the K15 negative cell. This result proved that, generally, cells with primary cilia were found around the basal cell area and a few number of ciliated cells also found in prickle cells around the basal area.

Statistical analysis of ciliated cell numbers was performed by capturing five random images on each skin sample taken around the basal cell area. The number of ciliated cells was divided by the total number of epidermal cells found in the single frame of the image. From the 15 samples of atopic dermatitis skin, the ciliated cell percentage number was significantly increase compared to normal skin from 8 different subjects, as shown in Figure 9a. Identically, skin samples of from eight different patients with psoriasis also showed a significant increase compare with normal skin as shown in Figure 10a. A previous study shows that cilia length may be influenced by some inflammatory cytokines[33]. The length of primary cilia found in atopic dermatitis and psoriasis skin was measured and compared with that in normal skin. However, no difference was found in

the length of primary cilia observed in normal, atopic dermatitis, and psoriasis skin samples (Figures 9b and 10b)

3.3 Observation of primary cilia formation in primary keratinocyte

Several studies related to skin inflammation, particularly regarding atopic dermatitis and psoriasis have been conducted and accommodated inflammation condition either *in vitro* or mimicking *in vivo* model [41–43]. However, these inflammation model were not deliberating the aspect of ciliogenesis in keratinocytes. Conversely, in recent studies, primary cilia or ciliary proteins in keratinocyte have been understood to pose a vital role related to cell activity and development[44,45]. By comparing atopic dermatitis and psoriasis skin samples with normal skin samples, I observed a significant increase in primary cilia formation in the epidermis area, as explained in the previous section. However, as a previous study reported, *in vitro* primary cilia formation in keratinocytes was not as high as other epithelial cells such as retinal pigment epithelium cell (RPE)[46]. In this study, primary keratinocyte culture was used for *in vitro* experiments to comprehend the role of primary cilia in skin inflammation. Initially, I observed the progression of primary cilia formation in keratinocytes. NHEK was cultured in serum starvation condition and the ciliogenesis was compared with normal serum condition in time point experiment. Serum starvation condition has been widely used to induce ciliogenesis in various kinds of cell[47]. The immunocytochemistry of primary cilia in NHEK was performed using a combination of antibody for fibroblast growth factor receptor 1 oncogene partner (FOP) which is the centrosomal protein in keratinocytes and anti-ARL13B antibody. The staining images in Figure 11 show time-dependent ciliogenesis observed in normal and serum-depleted cultures. For total 2-day experiment, an increase of ciliogenesis was observed after 24 h culture in a serum starvation condition. This increase steadily rises until 48 h of incubation

(Figure 12). Conversely, a decreasing trend of ciliogenesis was observed in normal serum conditions (Figure 12). A prolonged experiment of up to 6 days in serum starvation condition showed that maximum ciliogenesis occurred between 48 and 96 h (Figure 13a and b). This result may describe the temporal event of ciliogenesis in keratinocytes, which required around 2 to 4 days to exhibit the optimum formation of primary cilia. Regarding this result, I opted to culture NHEK in 2- or 3-days culture period for subsequent experiment in the analysis of ciliated keratinocyte on inflammation condition.

3.4 Stimulation using Th2 and Th17 cytokines increase ciliogenesis in primary keratinocyte but not with Th1 cytokines

As previously described, *in vitro* study of skin inflammation has been conducted by incubating primary keratinocytes using various cytokines and pro-inflammatory molecules[7,10,24]. However, the effect of keratinocyte stimulation using multiple cytokines in terms of ciliogenesis has not been performed previously. Regarding this situation, I attempted to check the effect of multiple cytokines stimulation at various concentrations on primary cilia formation in NHEK. Concentration range from 0 to 1000 ng/ml was used to stimulate NHEK for 48 h and the immunocytochemistry (ICC) staining was performed to analyze the primary cilia number based on quantitative analysis. The result was shown in Figure 15 for Th2 and Figure 17 for Th17 cytokines.

NHEK stimulation using Th2 cytokines (IL-4, IL-13, and IL-31) at various concentrations show increasing number of ciliated cells starting from smallest concentration of 1 ng/ml. However, the increase in ciliated cells did not follow concentration dependent manner. At high concentration, in particular starting from 200 ng/ml to 1000 ng/ml, ciliated cell number tend to be more stationed and finally decreased at the highest concentration

(Figure 15). In particular, 100 ng/ml of Th2 cytokines induced significant increase of ciliogenesis compared with control in NHEK culture as shown in ICC image and statistical analysis result in Figure 14a and b. Additionally, I also did not found any significant difference in cilia length after NHEK stimulation using IL-4, IL-13, and IL-31 (Figure 14c).

Figure 16 and Figure 17 describe the ciliogenesis in NHEK after stimulation using Th17 cytokines (IL-17A and IL-22). Concentration-dependent experiment showed the increasing tendency in ciliated cell number started to be observed in concentrations of 20 ng/ml for IL-17A and 1 ng/ml for IL-22 (Figure 17a and b). Similar to stimulation using Th2 (IL4/IL-13/IL-31), ciliated cell percentage after high concentration stimulation of Th17 cytokines (especially in the range of 200 to 1000 ng/ml) tends to be static or decreased (Fig. 17). Cilia staining image using anti-ARL13B antibody shown in red reveals significant increase in primary cilia after NHEK stimulation using 20 ng/ml of IL-17A and IL-22 for 48 h (Figure 16 a and b). IL-17A and IL-22 stimulation did not influence cilia length in NHEK culture either (Figure 16c).

Interestingly, the contrasting effect was shown after NHEK stimulation using Th1 cytokines (IL-1β, TNFα, and IFNγ). Forty-eight hours of stimulation in NHEK did not increase ciliated keratinocytes as shown from the ICC staining result and statistical analysis in Figure 18a and b. Furthermore, high concentrations of Th1 cytokines particularly TNFα and IFNγ induce negative effect on ciliogenesis as shown in Figure 19. No primary cilia were observed after NHEK stimulation using 100 ng/ml of TNFα and IFNγ (Figure 19b and c). Meanwhile change of IL-1β concentration seems to have minor impact on primary cilia increase (Figure 19a).

Regarding these results, I hypothesized that stimulation of NHEK using Th2 and Th17 cytokines, which were upregulated in atopic dermatitis and psoriasis, influenced primary cilia formation in primary keratinocyte culture. Although Th1 cytokines produced contrasting results, this outcome may explain the molecular mechanism of the increase in ciliated cells found in the epidermis of atopic dermatitis and psoriasis skin samples.

3.5 Downregulation of ciliary protein associated with differentiation protein, in particular desmoglein-1 and affected JNK signaling pathway in primary keratinocyte

The next concern is related to the impact of ciliogenesis increase in NHEK regarding the biological aspect of keratinocyte cell. To answer this condition, I made a cilia depleted model in NHEK by downregulating several cilia-related proteins. Earlier study has shown that ciliogenesis is influenced by not only IFT proteins but also a kinesin protein such as KIF3A[48]. I performed siRNA knockdown to inhibit several cilia-related proteins such as IFT88, KIF3A and ARL13B. Each siRNA contains sets (Table 2) of small RNA interference sequence and I selected the most effective sequence that gives maximum downregulation in mRNA level. Figure 20 describes the decreased mRNA expression level of IFT88, ARL13B and KIF3A. Although all sets of IFT88 gave optimum downregulatory outcome (Figure 20a), not all provided sequences of ARL13B and KIF3A inhibit the mRNA expression. Among them, siARL13B number 4 and siKIF3A number 2 gave maximum inhibition of mRNA expression (Figure 20b and c). Together with this particular sequence (siARL13B #2 and siKIF3A #4), I opted to use siIFT88 #2 in subsequent experiment to check the protein expression levels of IFT88, ARL13B, and KIF3A. Similar to quantitative real time PCR result, protein expression levels of IFT88, ARL13B, and KIF3A were decreased in comparison with either control or siRNA control

(Figure 21a-c). The effect of ciliary protein downregulation on primary cilia formation in NHEK is also shown using ICC image in Figure 21d and e. In this experiment, I used siIFT88 and IL-13 stimulation that represented the cause of primary cilia depletion and increase. Significant decrease in ciliated cell number was observed after siIFT88 treatment even after the stimulation of NHEK using IL-13 (Figure 21d and e). IFT88 was previously shown as an essential component in ciliogenesis[49]. Additionally, to mimic inflammation condition in general, IL-13 was used as it shows dominant factor found in atopic dermatitis but not in the lesional psoriasis[50].

Next, I performed a DNA microarray experiment using NHEK culture under ciliary protein (ARL13B, IFT88, or KIF3A) knockdown; with or without IL-13 stimulation for 48 h. Each treatment was compared with a control condition. By comparing the differentially expressed genes in keratinocyte after IL-13 stimulation and ciliary protein knockdown in IL-13 treated culture, I observed a total of 49 genes were associated with functional role of primary cilia (Figure 22 a and b; Table 4) These sets of genes related with the increase of primary cilia after stimulation of IL-13 in NHEK.

Among these genes, I found keratinocyte structural protein desmoglein-1 which is correlated with atopic dermatitis and pustular psoriasis pathophysiology[51,52]. Next I attempted to check desmoglein-1 expression in NHEK after IFT88 knockdown under inflammation cytokines stimulation. In this experiment, I also used Th17 cytokines (IL-17A and IL-22) besides IL-13 to represent the inflammation condition found in psoriasis. The knockdown of IFT88 significantly reduced the protein expression level compared with siCtrl even after cytokines stimulation, as shown by western blot result in Figure 23a and subsequent quantitative analysis in Figure 23b. Interestingly, I noticed that the downregulation of IFT88 affected the desmoglein-1 expression level in NHEK cells,

meanwhile stimulation with IL-13, IL-17A, and IL-22 showed a tendency to downregulate desmoglein-1 (Figure 23c and d).

Previous studies already showed that multiple signaling mechanisms modulate keratinocyte differentiation[53,54]. To understand the effect of primary cilia depletion (by IFT88 knockdown) and inflammatory cytokines stimulation (represented by IL-13) on signaling pathway cascade in keratinocytes, I run a bioplex experiment, which was able to screen multiple signaling protein expressions based on the immunoassay method. The screening revealed that a different pattern was found in the phosphorylation ratio of c-Jun and JNK, in which IL-13 stimulation increases the phosphorylation rate and downregulates after IFT88 knockdown (Figure 24c and d). Dissimilar results found in the ratio of AKT phosphorylation and another MAPK signaling phosphorylation, P38 (Figure 24a and b). Based on these results, I evaluated the effect of IL-13, IL-17A, and IL-22 stimulation and IFT88 downregulation on phosphorylated JNK. Time-dependent NHEK cell stimulation by Th2 (IL-13) and Th17 (IL-17A and IL-22) cytokines in conditions under which IFT88 was blocked were evaluated by western blot analysis (Figure 25a). Phosphorylated JNK expression was inhibited by abolishing IFT88 expression in NHEK cells, even after stimulation with cytokines for 48 h, which increases phosphorylated JNK, particularly IL-13 and IL-17A (Figure 25b). These inhibitory effects by IFT88 knockdown were not found in another MAPK pathway, phosphorylated P38 (Figure 26a and b). These findings suggest that JNK activation plays an essential role in skin inflammation. The present results indicate that JNK phosphorylation is modulated by IFT88 expression and may result from the primary cilia increase in atopic dermatitis and psoriasis.

3.6 Analysis of keratinocyte differentiation protein (Loricrin and Desmoglein-1) in regards with ciliated cell in the epidermis of normal, atopic dermatitis, and psoriasis skin sample

The next question to be addressed is the possible effect regarding the increase in ciliated cells found in the atopic dermatitis and psoriasis skin samples. In skin inflammation, keratinocyte differentiation is disturbed as a consequence of multiple molecular interplay[43]. In previous study, I found a correlation between ciliated cell number and loricrin expression in atopic dermatitis skin[35]. I sought a similar relationship using psoriasis skin sample. IHC staining of the psoriasis skin sample using anti-loricrin antibody was shown in red and primary cilia using anti-ARL13B antibody was shown in green as presented in Figure 27. Loricrin expression around the granular layer of the epidermis showed a strong signal in normal samples in which significantly low-almost no-ARL13B signal was found. Conversely, high number of primary cilia were observed in the psoriasis sample with a downregulated expression of Loricrin. However, both of these proteins were not colocalized since the dominant distribution of primary cilia was located around the basal layer whereas loricrin was expressed upon the granular layer of the epidermis.

I also sought alternative possibilities using another marker of keratinocyte differentiation. In the previous result section, I presented a plausible relationship between primary cilia (ciliary proteins) with desmoglein-1. Recently, desmoglein-1 has been associated with severe dermatitis and also found to be involved in pustular psoriasis[52,55]. Figure 28 shows the result of the desmoglein-1 expression level related to primary cilia number in normal, atopic dermatitis, and psoriasis skin samples. The solid expression of desmoglein-1 in normal skin presented in clear red, forming cell shape, which indicates desmoglein-1

function regarding cell-to-cell adhesion. However, in atopic dermatitis and psoriasis skin samples, this structure was not clearly found (Fig. 28, middle and right panels, second and third rows) despite increased cilia-like structure shown in the magnified images. However, primary cilia were found to not colocalize with desmoglein-1. The presentation of ciliated cell number and the expression of loricrin and desmoglein-1 in diseased skin compared with that in normal skin may point out the potential role of primary cilia in modulating keratinocyte differentiation, which is decimated in skin inflammation. Taken together, all of the obtained results may suggest a role for primary cilia in the epidermis.

4. Discussion

In the present study, observation of primary cilia in the normal and diseased skin samples together with *in vitro* experiments using primary keratinocytes revealed a probable role of primary cilia modulation in skin inflammation conditions. Ciliated keratinocyte increase was found around the basal layer of the epidermis in atopic dermatitis and psoriasis skin samples compared with that in normal skin samples. Additionally, increase of primary cilia found in diseased skin may associated with differentiation protein, loricrin and desmoglein-1 expression in the epidermis. An interesting finding was observed after NHEK stimulation using Th2 and Th17 cytokines, which significantly increased the number of ciliated cells. Furthermore, functional analysis of cilia-related protein suggested a plausible association of primary cilia to desmoglein-1 expression and phosphorylation of SAPK/JNK protein in primary keratinocytes. These results indicate a particular role of epidermal cilia related to the keratinocyte differentiation in skin inflammation pathophysiology.

4.1 Ciliated cell increase found around the basal cell layer in the epidermis of atopic dermatitis and psoriasis skin samples

Primary cilia are known to have essential function in skin development. Earlier study showed that primary cilia play a vital role in keratinocyte differentiation as the hub of important signaling pathways involved in the proliferation and differentiation of skin cells[48]. Primary cilia are also known to regulate Notch signaling in the basal layer and lower part of the suprabasal layer during epidermal development[56]. Moreover, keratinocyte cilia have an important function in skin homeostasis and may increase in response to environmental stress such as inflammation condition[31]. From previously

published research, primary cilia have shown a regulatory role for cell and tissue organization[57]. In addition, *intu*, an important gene for regulation of keratinocyte organization in the epidermis, also involved in the formation of primary cilia in keratinocyte[58]. Despite the discovery of primary cilia actions in the development and homeostasis of keratinocytes, the role of epidermal cilia in skin disorders remains unclear. The findings of this study indicate a significant increase in the number of primary cilia in the epidermal skin of patients with atopic dermatitis and those with psoriasis compared to those with normal skin.

Since primary cilia are known regulate multiple signaling cascades, it may have a substantial role in the pathophysiology of skin inflammation. Epidermal hyperplasia, which is one of clinical signs commonly found among atopic dermatitis and psoriasis patients, resulted from the overproliferation of keratinocyte in the epidermis[60]. Previous study pointed out that the activation of keratinocyte proliferation leads to epidermal hyperplasia through epidermal growth factor receptor (EGFR) modulation[61]. Primary cilia were known to regulate EGFR, and even in several organs, receptors that involved in EGFR signaling were found in primary cilia[62]. The findings from other reports supported a possibility of primary cilia role in skin inflammation related to EGFR regulation in keratinocyte. However, I could not find any clear change in EGFR and other related protein in the experiments.

4.2 Increase in ciliated cells also found after Th2 and Th17 cytokines stimulation in NHEK

To comprehend the process of primary cilia formation in keratinocyte, I cultured NHEK under serum starvation incubation. Serum starvation condition has shown to increase primary cilia formation in various kinds of cells[63]. Similarly, the induction of ciliated cells

in keratinocyte by increasing Ca^{2+} is also demonstrated in earlier study[64]. Since calcium also induces keratinocyte differentiation[28], I opted to omit this factor during keratinocyte stimulation using pro-inflammatory cytokines. Moreover, atopic dermatitis and psoriasis skin observation showed that most ciliated cells were found along the basal cell layer in which the differentiation is not the main phenotype of keratinocyte in this spatial circumstance[65]. In this study, I found that optimal primary cilia growth was observed in 24-48 h of incubation. This result was applied for the analysis of pro inflammatory cytokines stimulation on primary cilia formation in keratinocyte.

Recognized as the most common skin inflammation disorders, atopic dermatitis and psoriasis are characterized by inflammatory episodes leading to skin barrier destruction. The inflammation condition mainly is resulted from overexpressed pro-inflammatory cytokines such as Th1 cytokines (IL-1β, TNFα, and IFNγ) and Th2 cytokines (IL-4 and IL-13) particularly increased in atopic dermatitis, as well as Th17 cytokines (IL-17A and IL-22) increased in psoriasis. In this study, I found that stimulation of keratinocyte with IL-4, IL-13, IL-31, IL17A, and IL-22 significantly increase the primary cilia formation while Th1 cytokines (IL-1β, TNFα, and IFNγ) did not raise the ciliogenesis in keratinocyte. These result open a novel possibility of functional impact of pro-inflammatory cytokines in keratinocyte.

Multiple previous studies have demonstrated a significant role of Th2 cytokines in altering keratinocyte equilibrium. The activity of Th2 cytokines has been known to modulate the STAT pathway, undermining the keratinocyte structure and harming skin barrier functions[13,66–68]. Additionally, IL-13 had been recognized to present a principal role in atopic dermatitis[50]. Similarly, IL-17 and IL-22 stimulation has been shown to disrupt keratinocyte differentiation which reflects the pathophysiology of psoriasis[69,70].

Previous study revealed that the modulation of keratinocyte by cytokines lead to the disruption of proliferation-differentiation balance and delayed keratinocyte maturation[10,71,72]. Conversely, primary cilia are known to maintain keratinocyte homeostasis in keeping the stemness ability and to differentiate by producing structural protective protein[29]. Multiple signaling pathways are activated during skin inflammation. Increased in ciliated cells after Th2 and Th17 stimulation may have resulted from the modulation of various signaling cascades. I presented the association of IFT88, a substantial ciliogenesis protein, with the phosphorylation of JNK in keratinocytes (Fig. 25). Moreover, IL-13 and IL-17A increased JNK phosphorylation in keratinocyte as shown in Figure 25. Since JNK activation was found to be involved in EGFR modulation during epidermal morphogenesis[73], all of these factors may contribute to the promotion of cilia formation in keratinocytes.

4.3 IFT88, a substantial ciliary protein, presents an association with Desmoglein-1 and phosphorylation of JNK in primary keratinocytes

From this study, DNA array results showed a group of genes that were associated with the knockdown of mRNA involved in cilia formation and the effect of IL-13 stimulation in keratinocytes. Among that group, some notable gene related to keratinocyte differentiation proteins was found. Besides desmoglein-1, claudin-4 and corneodesmosin showed a plausible relation. This is an expected result since claudin-4 was found to be modulated in atopic dermatitis[74] and pathophysiology of atopic dermatitis and psoriasis is also known to modulate corneodesmosin expression[75,76]. Array analysis also pointed out fold difference for DUSP10 (Table 4), a dual-specificity phosphatase that is recognized to negatively modulate SAPK/JNK pathway[77]. In accordance with the

published result, screening of the affected signaling cascade also leads to a specific response shown by c-Jun and JNK phosphorylation based on Bioplex immunoanalysis.

Under specific circumstances, I found that blocking IFT88 expression modulates NHEK cell response to Th2 (IL-13) and Th17 (IL-17A and IL-22) cytokines stimulation by suppressing JNK phosphorylation. Inhibiting the JNK activity has been shown to promote keratinocyte differentiation[78]. As a differentiation protein, desmoglein-1 is identified to be negatively regulated by EGFR modulation[80]. Desmoglein-1 expression is found to decrease in severe atopic dermatitis[55]. In previous report, desmoglein-1 was shown to be involved in psoriasis associated with pemphigus foliaceus[52]. Additionally, IL-4 and IL-13 stimulation in NHEK was shown to release a peptidase class kallikren 7 (KLK7) which was straightly involved in degradation of desmoglein-1[81]. From the experiment in this reasearch, the stimulation of NHEK with IL-13, IL-17, and IL-22 were shown to decrease desmoglein-1 in both normal and IFT88 downregulated NHEK (Fig. 23, c-d). Since desmoglein-1 is known to modulate NHEK differentiation[79], this may explain the association of IFT88 downregulation, which leads to inhibit JNK phosphorylation, with increase in desmoglein-1 expression in NHEK.

The association of primary cilia increase with the downregulation of desmoglein-1 and loricrin was also found in skin inflammation samples, as shown in Figures 27 and 28. Although the co-staining of these keratinocyte structural protein was not found in the same location, this result might suggest the indirect role of primary cilia in keratinocyte differentiation. Different result found in the *in vitro* experiment using NHEK show the limitations of *in vitro* studies in terms of the spatial and temporal aspects of keratinocyte differentiation and proliferation programming.

Primary cilia increase that was found in the basal epidermis layer of atopic dermatitis and psoriasis skin samples may have been associated with the modulation of JNK pathway. Previous study has shown a substantial role of JNK in EGFR signaling, which altered keratinocyte differentiation and was involved in pathophysiology of skin inflammation[82]. Tight regulation of keratinocyte differentiation was known to be modulated by JNK signaling[83,84]. In this study, I demonstrated the relation of primary cilia increase with the downregulation of structural and terminal differentiation protein in atopic dermatitis and psoriasis. The JNK pathway is known to be a critical element in inflammatory skin disease, given that JNK is involved in multiple mechanisms which lead to gap junction and barrier protein deformation[85]. Previous studies have established that JNK-1 knockout mitigates the induction of atopic dermatitis in mice[86]. JNK activation has been found in psoriatic skin[87].

The high numbers of primary cilia discovered in the skin with atopic dermatitis and psoriasis in comparison with that of normal skin provide a novel feature for characterizing the phenomena of skin inflammation typically regarding keratinocyte differentiation. Given that primary cilia are crucial cell structures in signaling, they have an influential role in the alterations of skin architecture caused by stimulant exposure. To summarize, the modulation of JNK phosphorylation by IFT88 in Th2 and Th17 cytokine-stimulated NHEK cells is a hypothetical basis for the irregular ciliogenesis observed in atopic dermatitis and psoriasis, corresponding to a decline in keratinocyte maturation and the generation of defects in the skin structure (Figure 29). Various pharmaceutical products have been approved to improve the quality of life which is deteriorated in skin inflammation disease. However, none of them focusing in modulation of keratinocyte primary cilia. The findings in this study may contribute to the recognition of epidermal

cilia role in inflammation for development of novel atopic dermatitis and psoriasis therapeutic agent through modulation of keratinocyte differentiation.

Acknowledgment

The study was performed by direction of Prof. Fumihro Okada, Dr. Fumitaka Fujita, Dr. Manami Toriyama, and Dr. Hiroko Kato in Laboratory of Advance Cosmetic Science, Graduate School of Pharmaceutical Science, Osaka University. I would like present my utmost gratitude towards Prof. Okada, Dr. Fujita, Dr. Toriyama, and Dr. Kato for their sincere guidance, insightful suggestion, and unstoppable encouragement. They gave me a full opportunity and trust to establish this study. I also would like to express my appreciation for Prof. Akimichi Morita and Dr. Motoki Nakamura (Nagoya City University) for continuous advice and supporting with the skin samples. I would like to appreciate Prof. Ishii (The University of Tokyo) for substantial comment and suggestion on the experiment. I would like to present my indebtedness to Dr. Ryuichiro Kurata, Dr. Kaori Saito, Dr. Jun Usukura, Dr. Kie Nakashima, Dr. Tomohisa Hayakawa, Ayumi Terada, Yukari Fukunishi, all students and alumnus from laboratory for their full support and help during my study. I am also truly grateful to JICA, Mandom Corporation, and Bandung Institute of Technology for supporting and giving me the chance.

Finally, I would like to present my absolute gratefulness towards both of my parents and parents in law, my dearest wife and my children for their unconditional love, support and encouragement, thank you very much.

Osaka,

January 2021

References

1. Kabashima K. Immunology of the skin: Basic and clinical sciences in skin immune responses. Immunology of the Skin: Basic and Clinical Sciences in Skin Immune Responses. doi:10.1007/978-4-431-55855-2

2. Nestle FO, Di Meglio P, Qin JZ, Nickoloff BJ. Skin immune sentinels in health and disease. *Nat Rev Immunol*. 2009;9(10):679-691. doi:10.1038/nri2622

3. Kabashima K, Honda T, Ginhoux F, Egawa G. The immunological anatomy of the skin. *Nat Rev Immunol*. 2019;19(1):19-30. doi:10.1038/s41577-018-0084-5

4. Laggner U, Di Meglio P, Perera GK, et al. Identification of a Novel Proinflammatory Human Skin-Homing Vγ9Vδ2 T Cell Subset with a Potential Role in Psoriasis. *J Immunol*. 2011;187(5):2783-2793. doi:10.4049/jimmunol.1100804

5. Dijkgraaf FE, Matos TR, Hoogenboezem M, et al. Tissue patrol by resident memory CD8+ T cells in human skin. *Nat Immunol*. 2019;20(6):756-764. doi:10.1038/s41590-019-0404-3

6. Honda T, Kabashima K. Review Novel concept of iSALT (inducible skin-associated lymphoid tissue) in the elicitation of allergic contact dermatitis. doi:10.2183/pjab.92.20

7. Brandt EB, Sivaprasad U. Th2 Cytokines and Atopic Dermatitis. *J Clin Cell Immunol*. 2011;2(3). doi:10.4172/2155-9899.1000110

8. Nomura I, Goleva E, Howell MD, et al. Cytokine milieu of atopic dermatitis, as compared to psoriasis, skin prevents induction of innate immune response genes.

J Immunol. 2003;171(6):3262-3269. doi:10.4049/jimmunol.171.6.3262

9. Koga C, Kabashima K, Shiraishi N, Kobayashi M, Tokura Y. Possible pathogenic role of Th17 cells for atopic dermatitis. *J Invest Dermatol*. 2008;128(11):2625-2630. doi:10.1038/jid.2008.111

10. Bernard F-X, Morel F, Camus M, et al. Keratinocytes under Fire of Proinflammatory Cytokines: Bona Fide Innate Immune Cells Involved in the Physiopathology of Chronic Atopic Dermatitis and Psoriasis. *J Allergy*. 2012;2012:718725. doi:10.1155/2012/718725

11. Pasparakis M, Haase I, Nestle FO. Mechanisms regulating skin immunity and inflammation. *Nat Rev Immunol*. 2014;14(5):289-301. doi:10.1038/nri3646

12. Weidinger S, Novak N. Atopic dermatitis. *Lancet (London, England)*. 2016;387(10023):1109-1122. doi:10.1016/S0140-6736(15)00149-X

13. Hammad H, Lambrecht BN. Barrier Epithelial Cells and the Control of Type 2 Immunity. *Immunity*. 2015;43(1):29-40. doi:10.1016/J.IMMUNI.2015.07.007

14. Elias PM, Schmuth M. Abnormal skin barrier in the etiopathogenesis of atopic dermatitis. *Curr Opin Allergy Clin Immunol*. 2009;9(5):437-446. doi:10.1097/ACI.0b013e32832e7d36

15. Nutten S. Atopic Dermatitis: Global Epidemiology and Risk Factors. *Ann Nutr Metab*. 2015;66(1):8-16. doi:10.1159/000370220

16. Salimi M, Barlow JL, Saunders SP, et al. A role for IL-25 and IL-33–driven type-2 innate lymphoid cells in atopic dermatitis. *J Exp Med*. 2013;210(13):2939-2950. doi:10.1084/jem.20130351

17. Guttman-Yassky E, Suárez-Fariñas M, Chiricozzi A, et al. Broad defects in epidermal cornification in atopic dermatitis identified through genomic analysis. *J Allergy Clin Immunol*. 2009;124(6). doi:10.1016/j.jaci.2009.09.031

18. Proksch E, Fölster-Holst R, Jensen JM. Skin barrier function, epidermal proliferation and differentiation in eczema. *J Dermatol Sci*. 2006;43(3):159-169. doi:10.1016/j.jdermsci.2006.06.003

19. Guttman-Yassky E, Nograles KE, Krueger JG. Contrasting pathogenesis of atopic dermatitis and psoriasis - Part I: Clinical and pathologic concepts. In: *Journal of Allergy and Clinical Immunology*. Vol 127. Elsevier Ltd; 2011:1110-1118. doi:10.1016/j.jaci.2011.01.053

20. Irvine AD, McLean WHI, Leung DYM. Filaggrin Mutations Associated with Skin and Allergic Diseases. *N Engl J Med*. 2011;365(14):1315-1327. doi:10.1056/NEJMra1011040

21. Boehncke WH, Schön MP. Psoriasis. *Lancet*. 2015;386(9997):983-994. doi:10.1016/S0140-6736(14)61909-7

22. Man XY, Chen XB, Li W, et al. Analysis of epithelial-mesenchymal transition markers in psoriatic epidermal keratinocytes. *Open Biol*. 2015;5(8). doi:10.1098/rsob.150032

23. Martin DA, Towne JE, Kricorian G, et al. The emerging role of IL-17 in the pathogenesis of psoriasis: Preclinical and clinical findings. *J Invest Dermatol*. 2013;133(1):17-26. doi:10.1038/jid.2012.194

24. Kurtz E, Jacques SL, Blauvelt Heather Rizzo AL, Kagami S, Phillips KG.

Hyperplasia Is Dependent on IL-17A Mediated Psoriasis-Like Epidermal − IL-23. *J Immunol*. 2011;186:1495-1502. doi:10.4049/jimmunol.1001001

25. De Benedetto A, Kubo A, Beck LA. Skin Barrier Disruption: A Requirement for Allergen Sensitization? *J Invest Dermatol*. 2012;132:949-963. doi:10.1038/jid.2011.435

26. Castex-Rizzi N, Galliano MF, Aries MF, et al. In vitro approaches to pharmacological screening in the field of atopic dermatitis. *Br J Dermatol*. 2014;170(SUPPL. 1):12-18. doi:10.1111/bjd.13106

27. Bochénska K, Smolińska E, Moskot M, Jakóbkiewicz-Banecka J, Gabig-Cimińska M. Models in the research process of psoriasis. *Int J Mol Sci*. 2017;18(12). doi:10.3390/ijms18122514

28. Deyrieux AF, Wilson VG. In vitro culture conditions to study keratinocyte differentiation using the HaCaT cell line. *Cytotechnology*. 2007;54(2):77-83. doi:10.1007/s10616-007-9076-1

29. Ezratty E, Stokes N, Chai S, Shah A, Williams S, Fuchs E. Differentiation During Skin Development. *Cell*. 2011;145(7):1129-1141. doi:10.1016/j.cell.2011.05.030.A

30. Wheway G, Nazlamova L, Hancock JT. Signaling through the Primary Cilium. *Front Cell Dev Biol*. 2018;6:8. doi:10.3389/FCELL.2018.00008

31. Croyle MJ, Lehman JM, O'Connor AK, et al. Role of epidermal primary cilia in the homeostasis of skin and hair follicles. *J Cell Sci*. 2011;124(9):e1-e1. doi:10.1242/jcs.091256

32. Irigoin F, L. Badano J. Keeping the Balance Between Proliferation and Differentiation:The Primary Cilium. *Curr Genomics*. 2011;12(4):285-297. doi:10.2174/138920211795860134

33. Wann AKT, Chapple JP, Knight MM. The primary cilium influences interleukin-1β-induced NFκB signalling by regulating IKK activity. *Cell Signal*. 2014;26(8):1735-1742. doi:10.1016/j.cellsig.2014.04.004

34. Baek H, Shin HJ, Kim J-J, et al. Primary cilia modulate TLR4-mediated inflammatory responses in hippocampal neurons. *J Neuroinflammation*. 2017;14(1):189. doi:10.1186/s12974-017-0958-7

35. Toriyama M, Rizaldy D, Nakamura M, et al. Immunological role of primary cilia of dendritic cells in human skin disease. *bioRxiv*. January 2020:2020.02.04.933333. doi:10.1101/2020.02.04.933333

36. Wong SY, Seol AD, So PL, et al. Primary cilia can both mediate and suppress Hedgehog pathway-dependent tumorigenesis. *Nat Med*. 2009;15(9):1055-1061. doi:10.1038/nm.2011

37. Sipos É, Komoly S, Ács P. Quantitative Comparison of Primary Cilia Marker Expression and Length in the Mouse Brain. *J Mol Neurosci*. 2018;64(3):397-409. doi:10.1007/s12031-018-1036-z

38. Thorpe SD, Gambassi S, Thompson CL, Chandrakumar C, Santucci A, Knight MM. Reduced primary cilia length and altered Arl13b expression are associated with deregulated chondrocyte Hedgehog signaling in alkaptonuria. *J Cell Physiol*. 2017;232(9):2407-2417. doi:10.1002/jcp.25839

39. Ritter A, Friemel A, Kreis NN, et al. Primary Cilia Are Dysfunctional in Obese Adipose-Derived Mesenchymal Stem Cells. *Stem Cell Reports*. 2018;10(2):583-599. doi:10.1016/j.stemcr.2017.12.022

40. Blanpain C, Fuchs E. Epidermal Stem Cells of the Skin. *Annu Rev Cell Dev Biol*. 2006;22(1):339-373. doi:10.1146/annurev.cellbio.22.010305.104357

41. Castex-Rizzi N, Galliano MF, Aries MF, et al. *In vitro* approaches to pharmacological screening in the field of atopic dermatitis. *Br J Dermatol*. 2014;170:12-18. doi:10.1111/bjd.13106

42. Welss T, Basketter DA, Schröder KR. In vitro skin irritation: Facts and future. State of the art review of mechanisms and models. *Toxicol Vitr*. 2004;18(3):231-243. doi:10.1016/j.tiv.2003.09.009

43. Van Den Bogaard EH, Tjabringa GS, Joosten I, et al. Crosstalk between keratinocytes and T cells in a 3D microenvironment: A model to study inflammatory skin diseases. *J Invest Dermatol*. 2014;134(3):719-727. doi:10.1038/jid.2013.417

44. Delaval B, Bright A, Lawson N, Doxsey S. The cilia protein IFT88 is required for spindle orientation in mitosis. *Nat Cell Biol*. 2011;13(4):461-468. doi:10.1038/ncb2202.The

45. Boehlke C, Janusch H, Hamann C, et al. A cilia independent role of Ift88/polaris during cell migration. *PLoS One*. 2015;10(10):1-19. doi:10.1371/journal.pone.0140378

46. Choi YJ, Laclef C, Yang N, et al. RPGRIP1L is required for stabilizing

epidermal keratinocyte adhesion through regulating desmoglein endocytosis. *PLoS Genet*. 2019;15(1). doi:10.1371/journal.pgen.1007914

47. Mirvis M, Stearns T, Nelson WJ. Cilium structure, assembly, and disassembly regulated by the cytoskeleton. *Biochem J*. 2018;475(14):2329-2353. doi:10.1042/BCJ20170453

48. Ezratty EJ, Stokes N, Chai S, Shah AS, Williams SE, Fuchs E. A Role for the Primary Cilium in Notch Signaling and Epidermal Differentiation during Skin Development. *Cell*. 2011;145(7):1129-1141. doi:10.1016/J.CELL.2011.05.030

49. Robert A, Margall-Ducos G, Guidotti J-E, et al. The intraflagellar transport component IFT88/polaris is a centrosomal protein regulating G1-S transition in non-ciliated cells. *J Cell Sci*. 2007;120:918. doi:10.1242/jcs.03422

50. Tsoi LC, Rodriguez E, Degenhardt F, et al. Atopic Dermatitis Is an IL-13-Dominant Disease with Greater Molecular Heterogeneity Compared to Psoriasis. *J Invest Dermatol*. 2019;139(7):1480-1489. doi:10.1016/j.jid.2018.12.018

51. McAleer MA, Pohler E, Smith FJD, et al. Severe dermatitis, multiple allergies, and metabolic wasting syndrome caused by a novel mutation in the N-terminal plakin domain of desmoplakin. *J Allergy Clin Immunol*. 2015;136(5):1268-1276. doi:10.1016/j.jaci.2015.05.002

52. de Sousa VB, Santana CNL e. L, Pereira D do N, Gripp AC. Pemphigus foliaceus with pustular presentation in a patient with psoriasis. *An Bras Dermatol*. 2017;92(5):115-117. doi:10.1590/abd1806-4841.20175709

53. Rangarajan A, Talora C, Okuyama R, et al. Notch signaling is a direct

determinant of keratinocyte growth arrest and entry into differentiation. *EMBO J*. 2001;20(13):3427-3436. doi:10.1093/emboj/20.13.3427

54. Calautti E, Li J, Saoncella S, Brissette JL, Goetinck PF. Phosphoinositide 3-kinase signaling to Akt promotes keratinocyte differentiation versus death. *J Biol Chem*. 2005;280(38):32856-32865. doi:10.1074/jbc.M506119200

55. Samuelov L, Sarig O, Harmon RM, et al. Desmoglein 1 deficiency results in severe dermatitis, multiple allergies and metabolic wasting. *Nat Genet*. 2013;45(10):1244-1248. doi:10.1038/ng.2739

56. Ezratty EJ, Pasolli HA, Fuchs E. A Presenilin-2-ARF4 trafficking axis modulates Notch signaling during epidermal differentiation. *J Cell Biol*. 2016;214(1):89-101. doi:10.1083/jcb.201508082

57. De Andrea CE, Wiweger M, Prins F, Bovée JVMG, Romeo S, Hogendoorn PCW. Primary cilia organization reflects polarity in the growth plate and implies loss of polarity and mosaicism in osteochondroma. *Lab Investig*. 2010;90(7):1091-1101. doi:10.1038/labinvest.2010.81

58. Dai D, Li L, Huebner A, et al. Planar cell polarity effector gene Intu regulates cell fate-specific differentiation of keratinocytes through the primary cilia. *Cell Death Differ*. 2013;20(1):130-138. doi:10.1038/cdd.2012.104

59. Hua K, Ferland RJ. Fixation methods can differentially affect ciliary protein immunolabeling. *Cilia*. 2017;6(1):5. doi:10.1186/s13630-017-0045-9

60. Noda S, Suárez-Fariñas M, Ungar B, et al. The Asian atopic dermatitis phenotype combines features of atopic dermatitis and psoriasis with increased TH17

polarization. *J Allergy Clin Immunol*. 2015;136(5):1254-1264. doi:10.1016/j.jaci.2015.08.015

61. El-Abaseri TB, Putta S, Hansen LA. Ultraviolet irradiation induces keratinocyte proliferation and epidermal hyperplasia through the activation of the epidermal growth factor receptor. *Carcinogenesis*. 2006;27(2):225-231. doi:10.1093/carcin/bgi220

62. Christensen ST, Clement CA, Satir P, Pedersen LB. Primary cilia and coordination of receptor tyrosine kinase (RTK) signalling. *J Pathol*. 2012;226(2):172-184. doi:10.1002/path.3004

63. Inoko A, Matsuyama M, Goto H, et al. Trichoplein and Aurora A block aberrant primary cilia assembly in proliferating cells. *J Cell Biol*. 2012;197(3):391-405. doi:10.1083/jcb.201106101

64. Lee CW, Lin ZC, Hu SCS, et al. Urban particulate matter down-regulates filaggrin via COX2 expression/PGE2 production leading to skin barrier dysfunction. *Sci Rep*. 2016;6(1):1-16. doi:10.1038/srep27995

65. Eckert RL, Efimova T, Dashti SR, et al. Keratinocyte survival, differentiation, and death: Many roads lead to mitogen-activated protein kinase. In: *Journal of Investigative Dermatology Symposium Proceedings*. Vol 7. Blackwell Publishing Inc.; 2002:36-40. doi:10.1046/j.1523-1747.2002.19634.x

66. Kim BE, Leung DYM, Boguniewicz M, Howell MD. Loricrin and involucrin expression is down-regulated by Th2 cytokines through STAT-6. *Clin Immunol*. 2008;126(3):332-337. doi:10.1016/j.clim.2007.11.006

67. Howell MD, Kim BE, Gao P, et al. Cytokine modulation of atopic dermatitis filaggrin skin expression. *J Allergy Clin Immunol*. 2007;120(1):150-155. doi:10.1016/j.jaci.2007.04.031

68. Howell MD, Fairchild HR, Kim BE, et al. Th2 Cytokines Act on S100/A11 to Downregulate Keratinocyte Differentiation. *J Invest Dermatol*. 2008;128(9):2248-2258. doi:10.1038/JID.2008.74

69. Boniface K, Bernard F-X, Garcia M, Gurney AL, Lecron J-C, Morel F. IL-22 Inhibits Epidermal Differentiation and Induces Proinflammatory Gene Expression and Migration of Human Keratinocytes. *J Immunol*. 2005;174(6):3695-3702. doi:10.4049/jimmunol.174.6.3695

70. Nograles KE, Zaba LC, Guttman-Yassky E, et al. Th17 cytokines interleukin (IL)-17 and IL-22 modulate distinct inflammatory and keratinocyte-response pathways. *Br J Dermatol*. 2008;159(5):1092-1102. doi:10.1111/j.1365-2133.2008.08769.x

71. Hänel KH, Cornelissen C, Lüscher B, Baron JM. Cytokines and the skin barrier. *Int J Mol Sci*. 2013;14(4):6720-6745. doi:10.3390/ijms14046720

72. Noske K. Secreted immunoregulatory proteins in the skin. *J Dermatol Sci*. 2018;89(1):3-10. doi:10.1016/j.jdermsci.2017.10.008

73. Weston CR, Wong A, Hall JP, Goad MEP, Flavell RA, Davis RJ. The c-Jun NH2-terminal kinase is essential for epidermal growth factor expression during epidermal morphogenesis. *Proc Natl Acad Sci U S A*. 2004;101(39):14114-14119. doi:10.1073/pnas.0406061101

74. Gruber R, Börnchen C, Rose K, et al. Diverse Regulation of Claudin-1 and Claudin-4 in Atopic Dermatitis. *Am J Pathol*. 2015;185(10):2777-2789. doi:10.1016/J.AJPATH.2015.06.021

75. Oji V, Eckl KM, Aufenvenne K, et al. Loss of corneodesmosin leads to severe skin barrier defect, pruritus, and atopy: Unraveling the peeling skin disease. *Am J Hum Genet*. 2010;87(2):274-281. doi:10.1016/j.ajhg.2010.07.005

76. Allen M, Ishida-Yamamoto A, Mcgrath J, et al. *Corneodesmosin Expression in Psoriasis Vulgaris Differs from Normal Skin and Other Inflammatory Skin Disorders*.; 2001.

77. Jiménez-Martínez M, Stamatakis K, Fresno M. The dual-specificity phosphatase 10 (DUSP10): Its role in cancer, inflammation, and immunity. *Int J Mol Sci*. 2019;20(7). doi:10.3390/ijms20071626

78. Gazel A, Banno T, Walsh R, Blumenberg M. Inhibition of JNK promotes differentiation of epidermal keratinocytes. *J Biol Chem*. 2006;281(29):20530-20541. doi:10.1074/jbc.M602712200

79. Hammers CM, Stanley JR. Desmoglein-1, differentiation, and disease. *J Clin Invest*. 2013;123(4):1419-1422. doi:10.1172/JCI69071

80. Sotiropoulou PA, Blanpain C. Development and homeostasis of the skin epidermis. *Cold Spring Harb Perspect Biol*. 2012;4(7):1-9. doi:10.1101/cshperspect.a008383

81. Morizane S, Yamasaki K, Kajita A, et al. TH2 cytokines increase kallikrein 7 expression and function in patients with atopic dermatitis. *J Allergy Clin*

Immunol. 2012;130(1):259. doi:10.1016/j.jaci.2012.03.006

82. Pastore S, Giustizieri ML, Mascia F, Giannetti A, Kaushansky K, Girolomoni G. Dysregulated activation of activator protein 1 in keratinocytes of atopic dermatitis patients with enhanced expression of granulocyte/macrophage-colony stimulating factor. *J Invest Dermatol*. 2000;115(6):1134-1143. doi:10.1046/j.1523-1747.2000.00149.x

83. You H, Padmashali RM, Ranganathan A, et al. JNK regulates compliance-induced adherens junctions formation in epithelial cells and tissues. doi:10.1242/jcs.122903

84. Schumacher M, Schuster C, Rogon ZM, et al. Efficient keratinocyte differentiation strictly depends on JNK-induced soluble factors in fibroblasts. *J Invest Dermatol*. 2014;134(5):1332-1341. doi:10.1038/jid.2013.535

85. Hammouda MB, Ford AE, Liu Y, Zhang JY. The JNK Signaling Pathway in Inflammatory Skin Disorders and Cancer. *Cells*. 2020;9(4):857. doi:10.3390/cells9040857

86. Choi J, Kim JR, Kim H, et al. The atopic dermatitis-like symptoms induced by MC903 were alleviated in JNK1 knockout mice. *Toxicol Sci*. 2013;136(2):443-449. doi:10.1093/toxsci/kft215

87. Takahashi H, Ibe M, Nakamura S, Ishida-Yamamoto A, Hashimoto Y, Iizuka H. Extracellular regulated kinase and c-Jun N-terminal kinase are activated in psoriatic involved epidermis. *J Dermatol Sci*. 2002;30(2):94-99. doi:10.1016/S0923-1811(02)00064-6

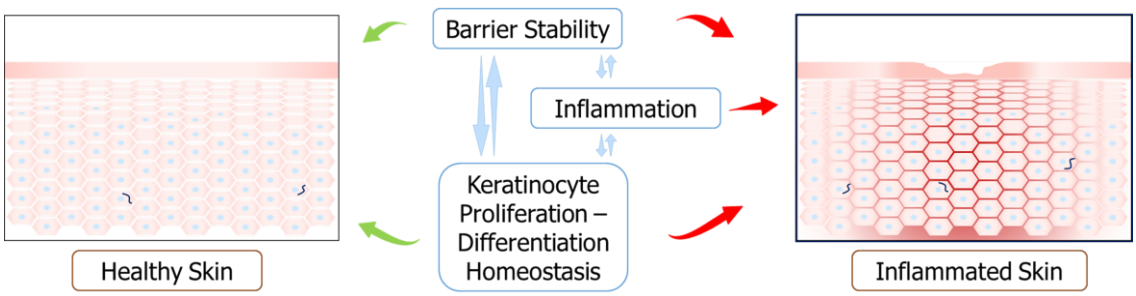

Figure 1.1 Inter-correlated relationship between skin protective function, activation of immune response, and maintenance of keratinocyte supporting epidermal morphogenesis. Disturbance to one of these component lead to initiate inflammation.

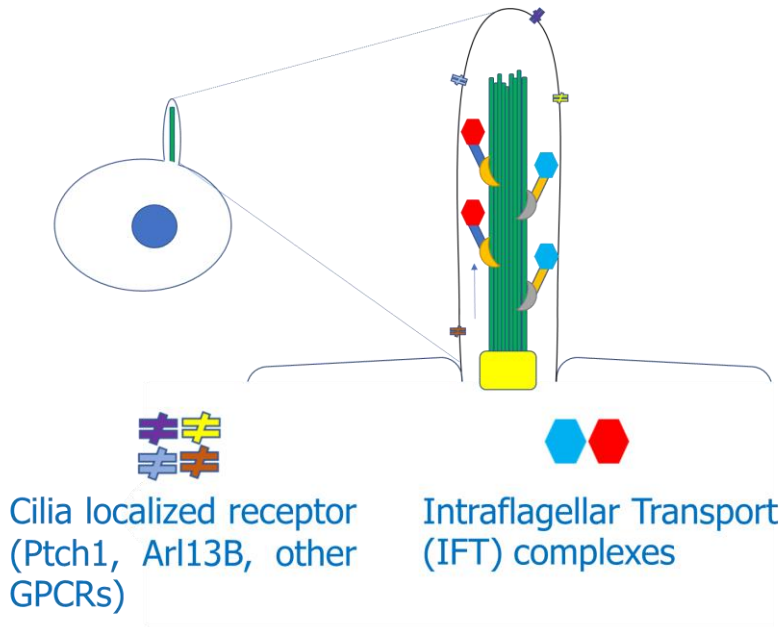

Figure 1.2 Simple illustration of primary cilia

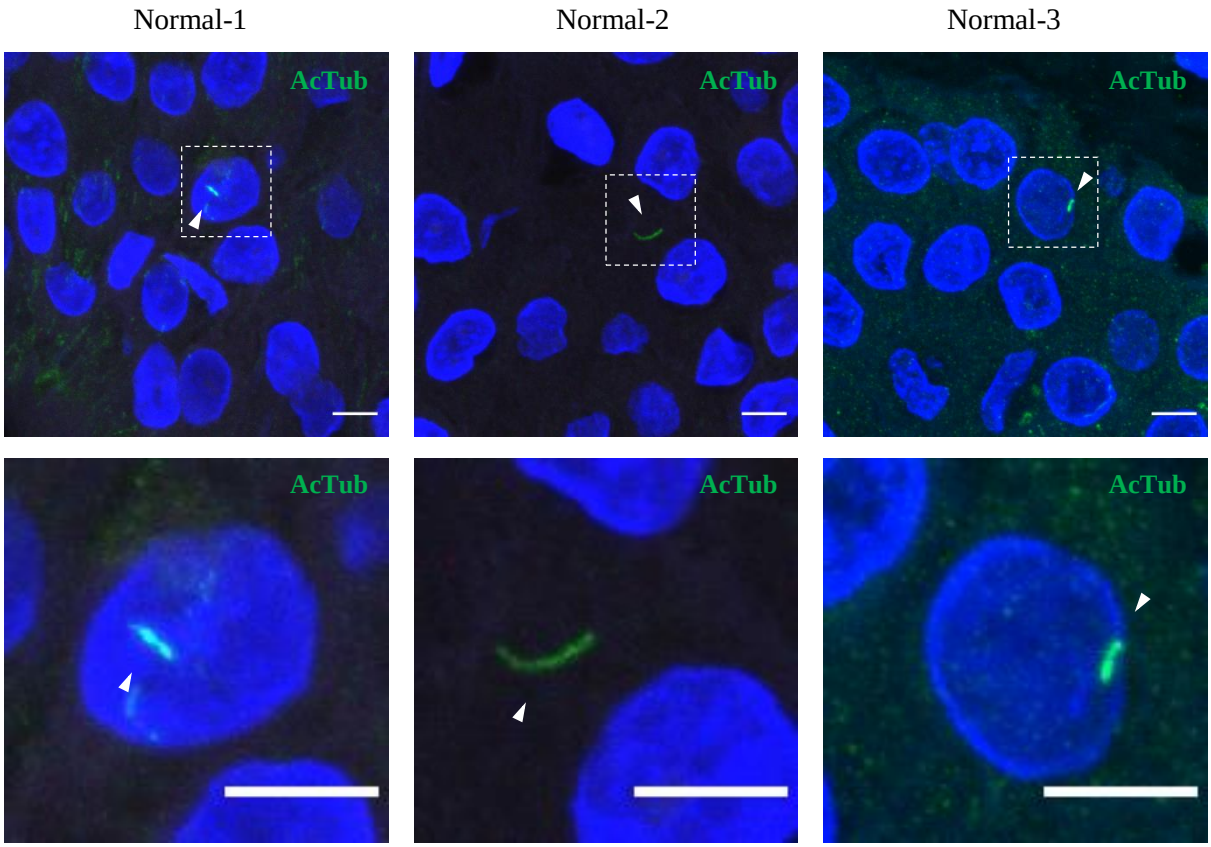

Figure 1
Fluorescent IHC image of normal skin, stained using anti-Acetylated α Tubulin (Green). The box indicated the enlarged area shown in the picture on the upper side. Arrowheads show primary cilia. Scale bar 5 µm.

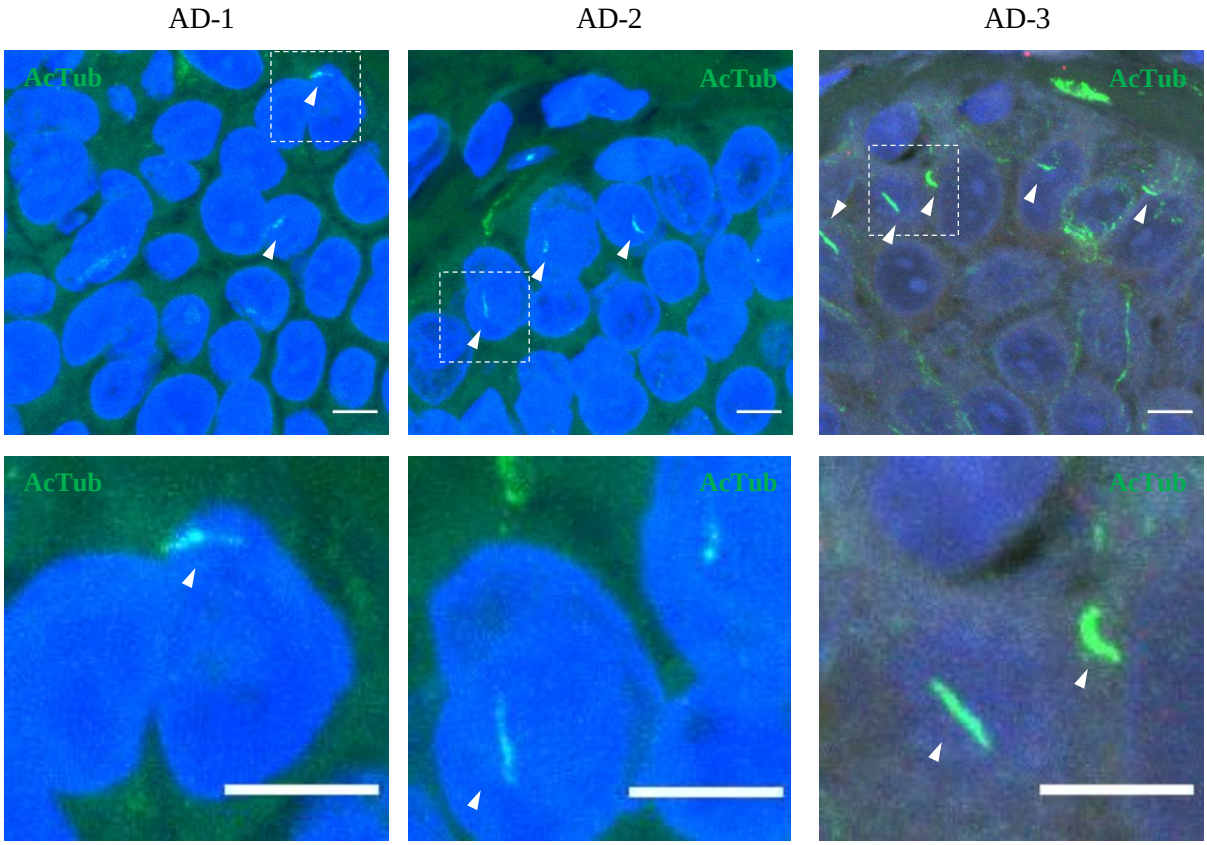

Figure 2
Fluorescent IHC image of atopic dermatitis skin, stained using anti-Acetylated α Tubulin (Green). The box indicated the enlarged area shown in the picture on the upper side. Arrowheads show primary cilia. Scale bar 5 μm.

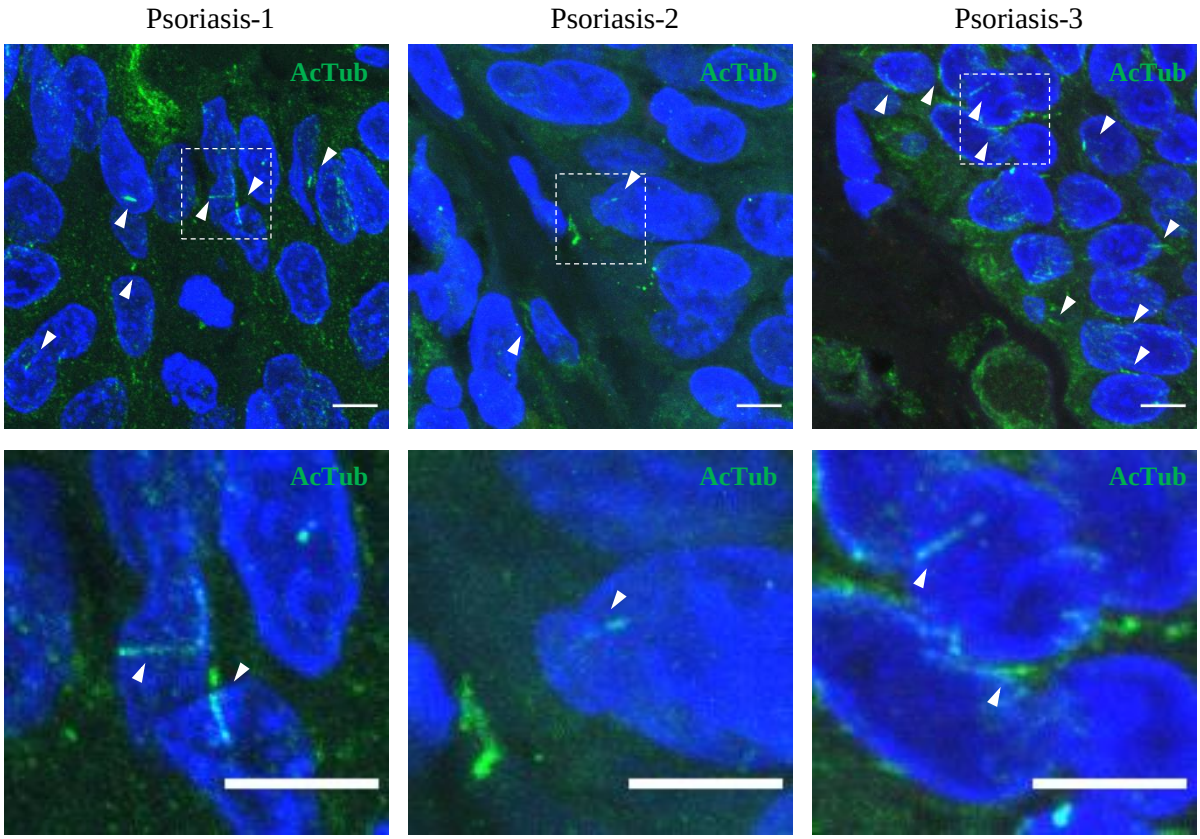

Figure 3
Fluorescent IHC image of psoriasis skin, stained using anti-Acetylated α Tubulin (Green). The box indicated the enlarged area shown in the picture on the upperside Arrowheads show primary cilia. Scale bar 5 µm.

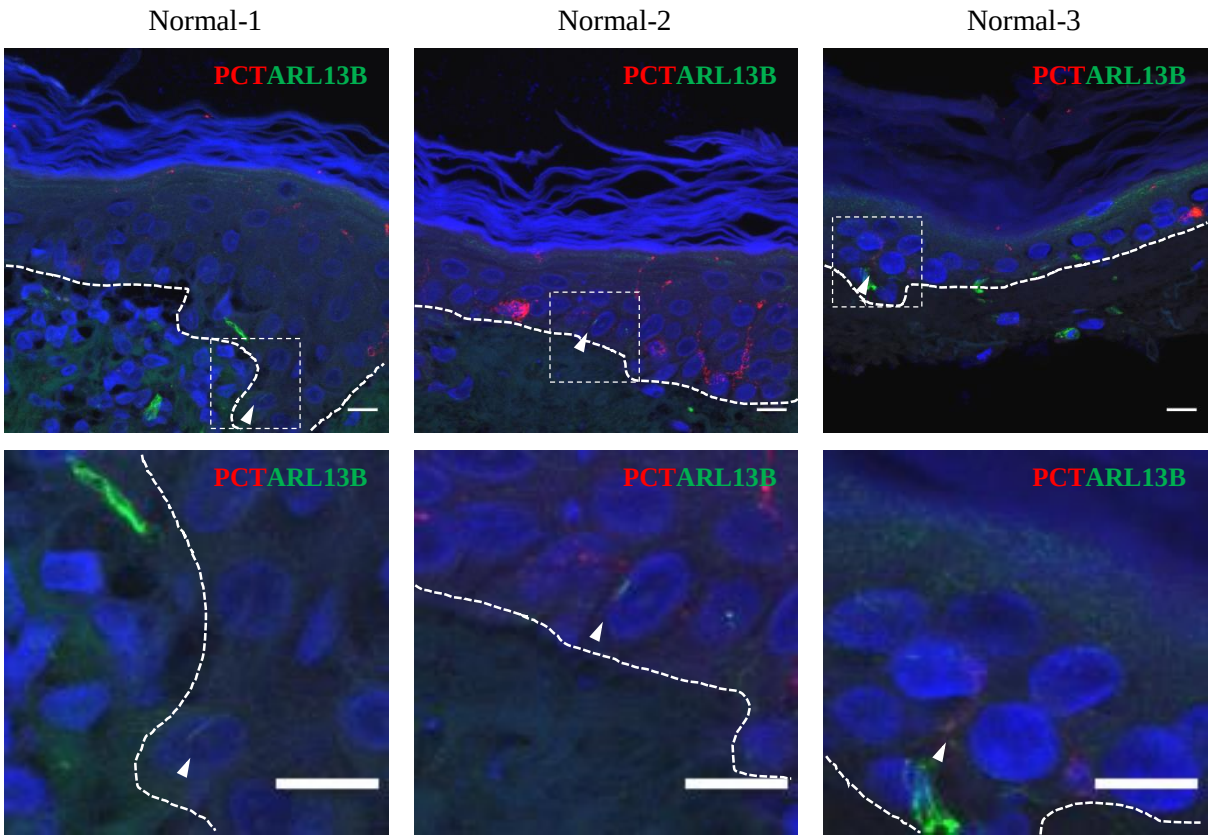

Figure 4
Fluorescent IHC image of normal skin, stained using anti-Pericentrin (Red) and anti-ARL13B (Green). White dash shows the basal line, upper part of the dash indicates the epidermis whereas dermis area located below the dash. The box indicated the enlarged area shown in the picture on the upper side. Arrowheads show primary cilia. Scale bar 10 µm.

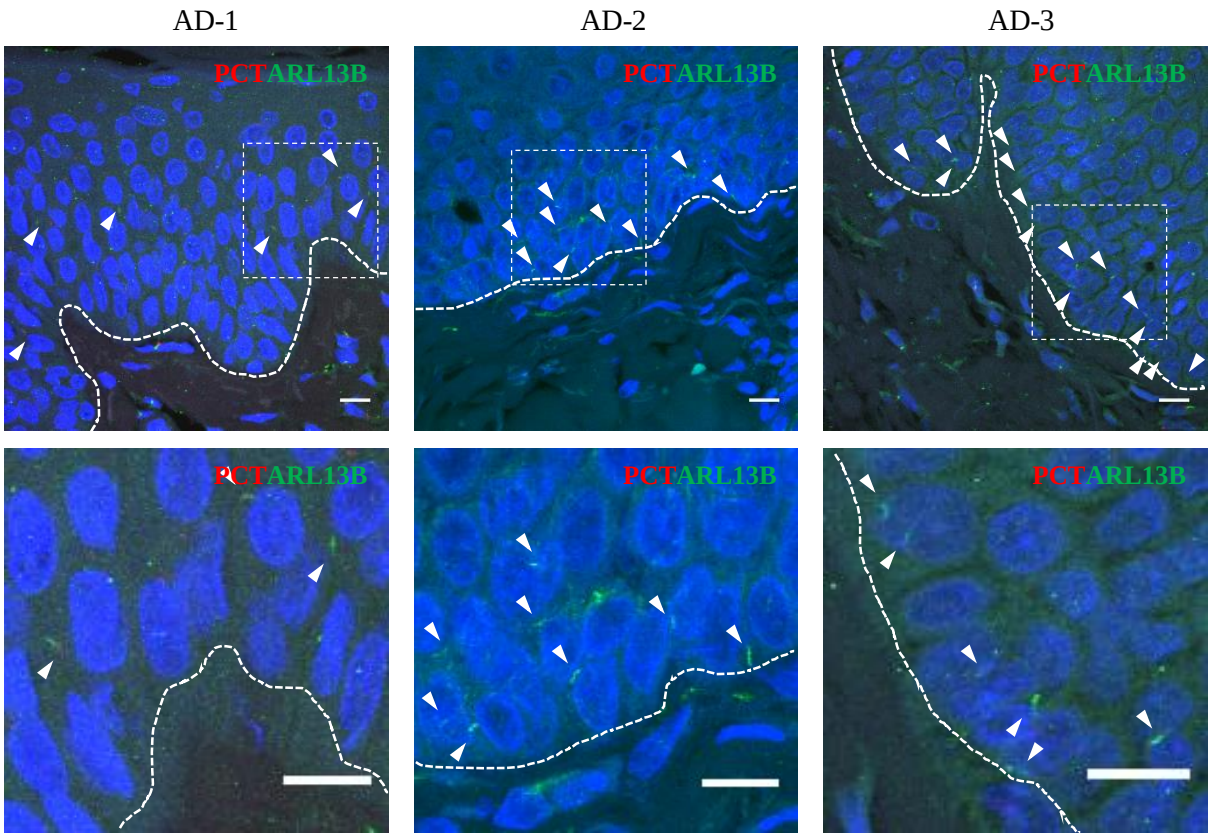

Figure 5
Fluorescent IHC image of atopic dermatitis skin, stained using anti-Pericentrin (Red) and anti-ARL13B (Green). White dash shows the basal line, upper part of the dash indicates the epidermis whereas dermis area located below the dash. The box indicated the enlarged area shown in the picture on the upper side. Arrowheads show primary cilia. Scale bar 10 µm.

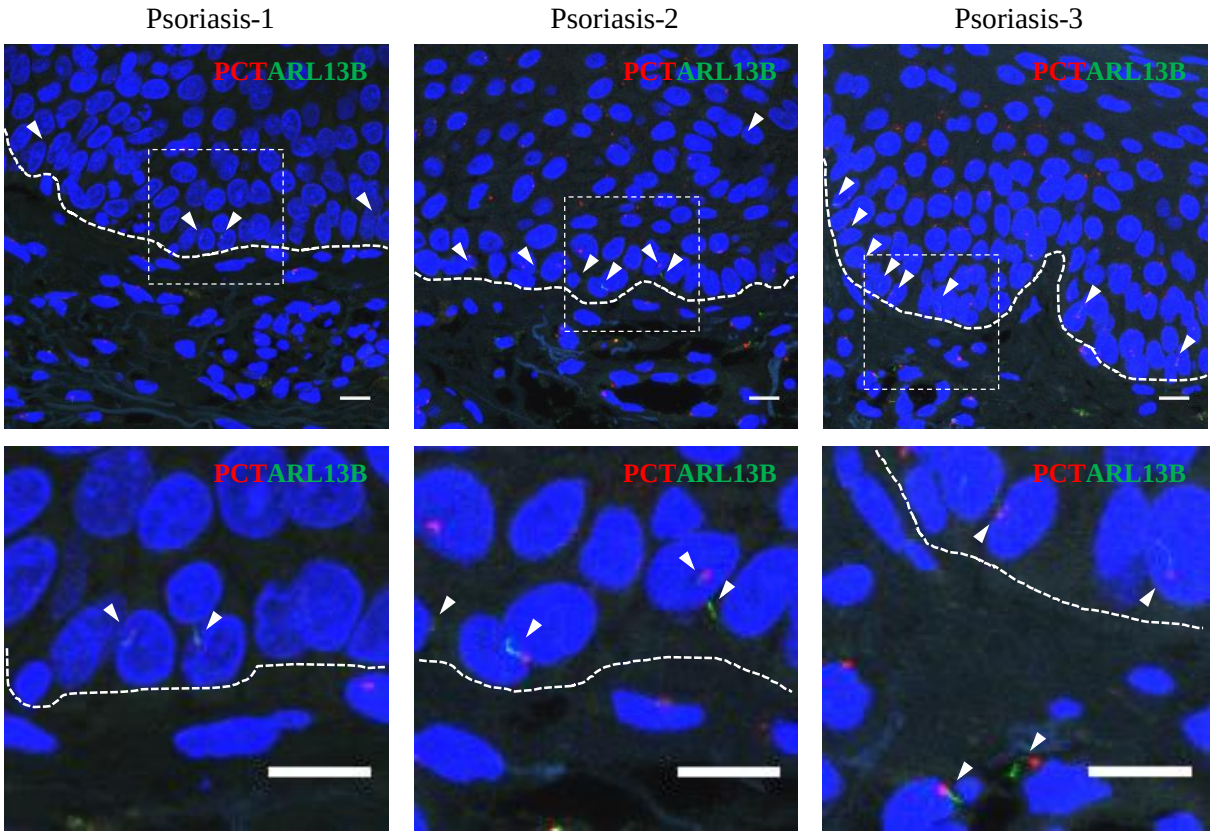

Figure 6
Fluorescent IHC image of psoriasis skin, stained using anti-Pericentrin (Red) and anti-ARL13B (Green). White dash shows the basal line, upper part of the dash indicates the epidermis whereas dermis area located below the dash. The box indicated the enlarged area shown in the picture on the upper side. Arrowheads show primary cilia. Scale bar 10 µm.

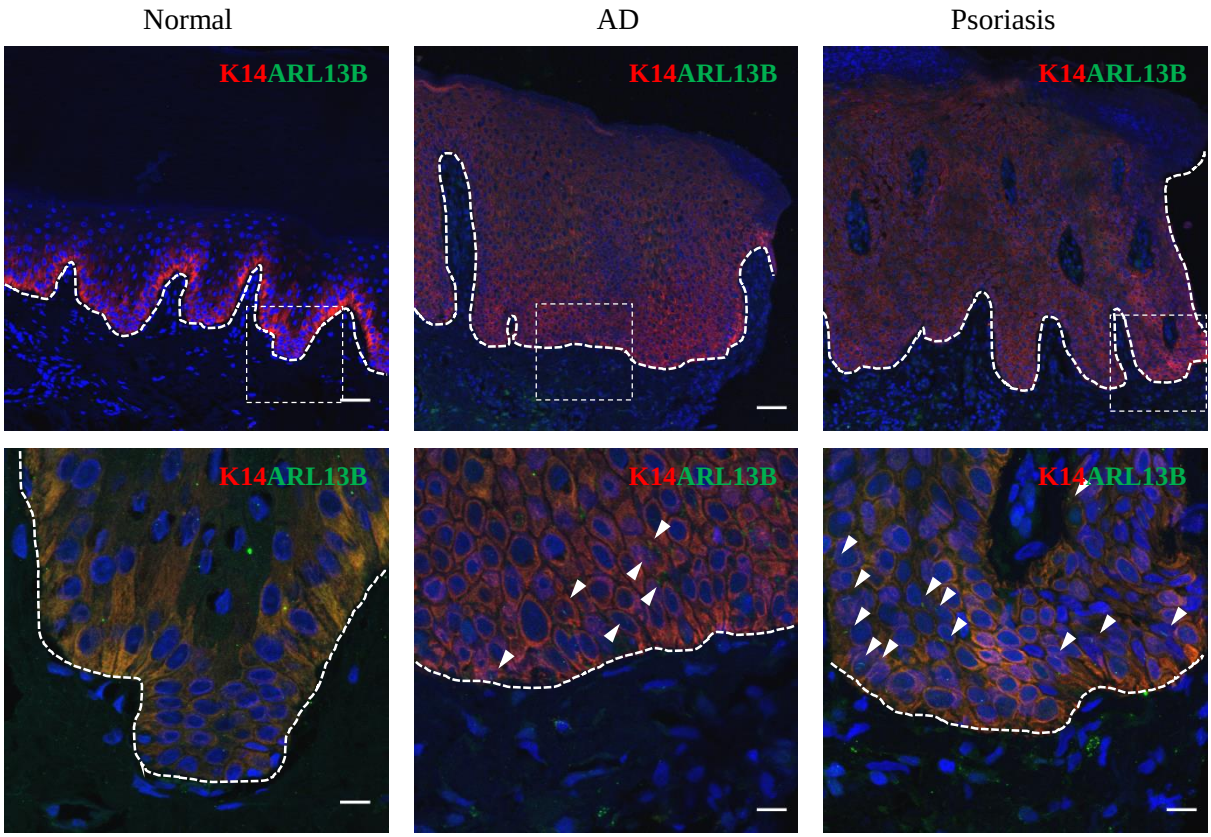

Figure 7
Fluorescent IHC image of normal, AD, and psoriasis skin, stained using anti-K14 (Red) and anti-ARL13B (Green). White dash shows the basal line, upper part of the dash indicates the epidermis whereas dermis area located below the dash. The box indicated the enlarged area shown in the picture on the upper side. Arrowheads show primary cilia. Scale bar 50 µm (upper panel) 10 µm (lower panel).

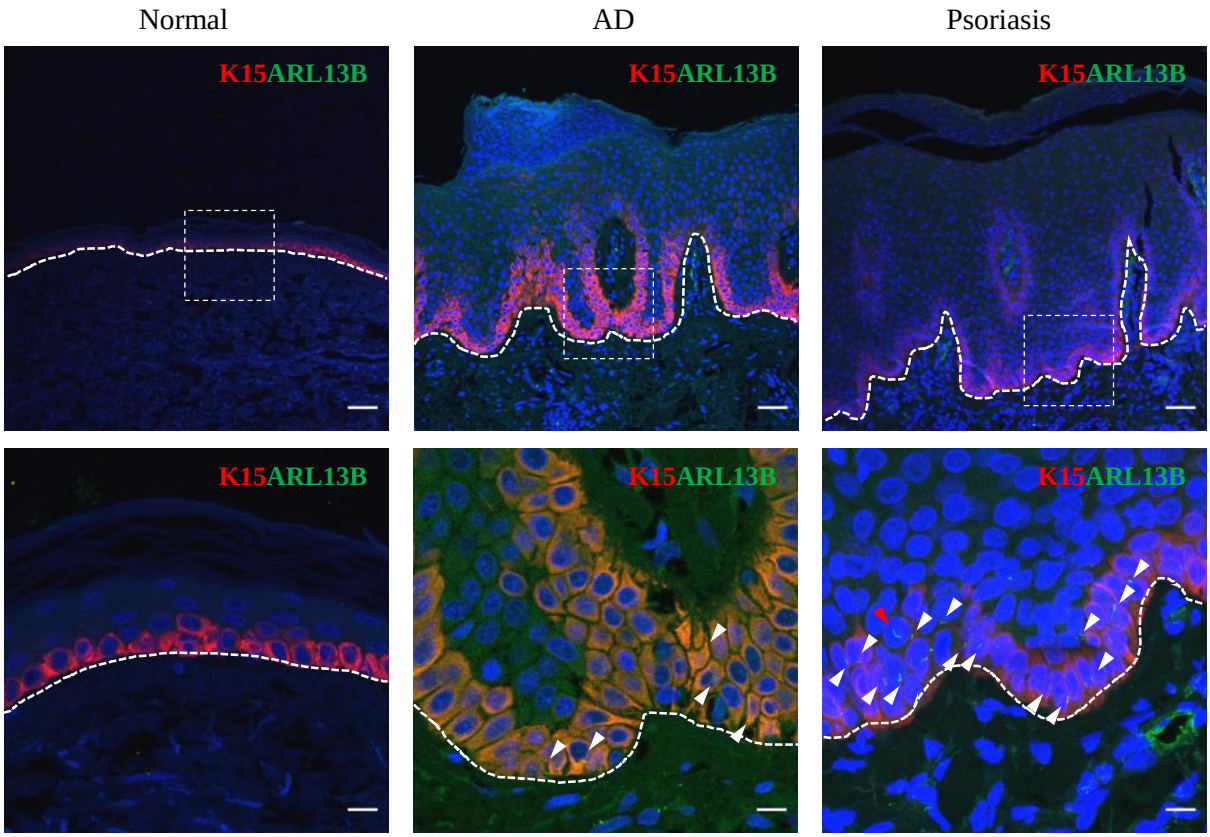

Figure 8
Fluorescent IHC image of normal, AD, and psoriasis skin, stained using anti-K15 (Red) and anti-ARL13B (Green). White dash shows the basal line, upper part of the dash indicates the epidermis whereas dermis area located below the dash. The box indicated the enlarged area shown in the picture on the upper side. Arrowheads show primary cilia. Scale bar 50 µm (upper panel) 10 µm (lower panel).

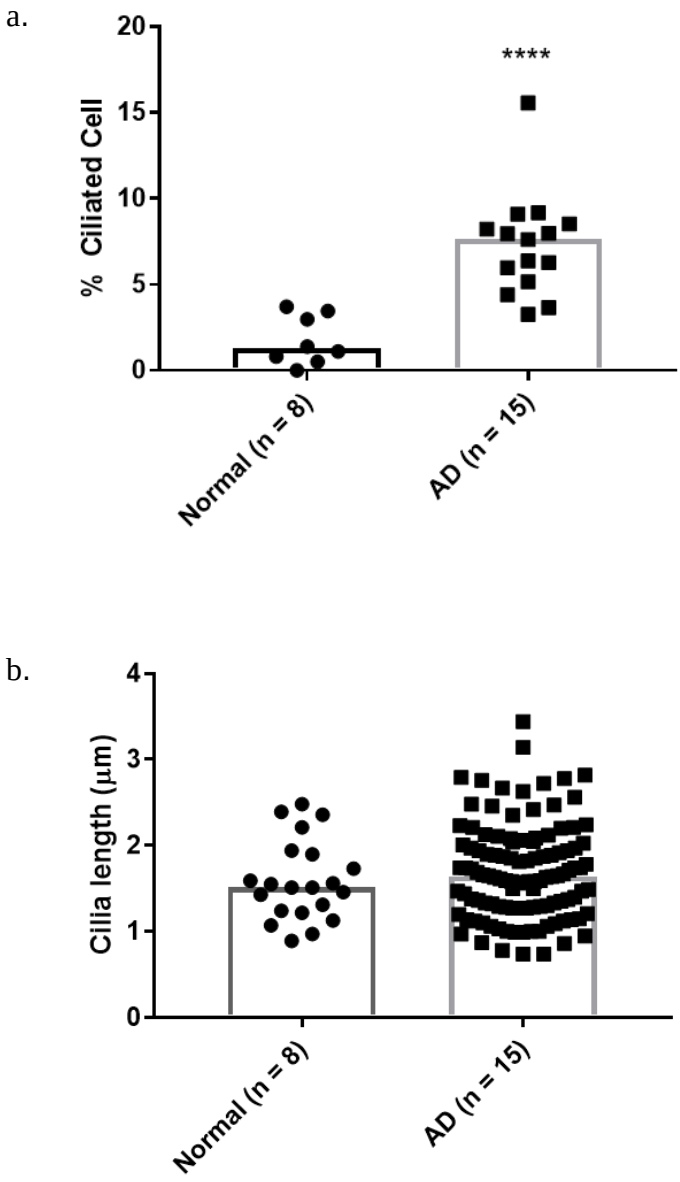

Figure 9

(a) Statistical analysis of ciliated cell percentage calculation in normal and AD skin. About 500–700 cells from several locations of epidermal area were observed using confocal imaging. The number of primary cilia and cells in each picture were counted using ImageJ. Bar graph shows median. **** $P < 0.0001$ (Mann Whitney U-Test). (b) Length of primary cilia both in normal and AD skin. Approximately 500–700 cells from several locations of epidermal area were observed using confocal imaging, lengths of observed cilia were measured using ImageJ software.

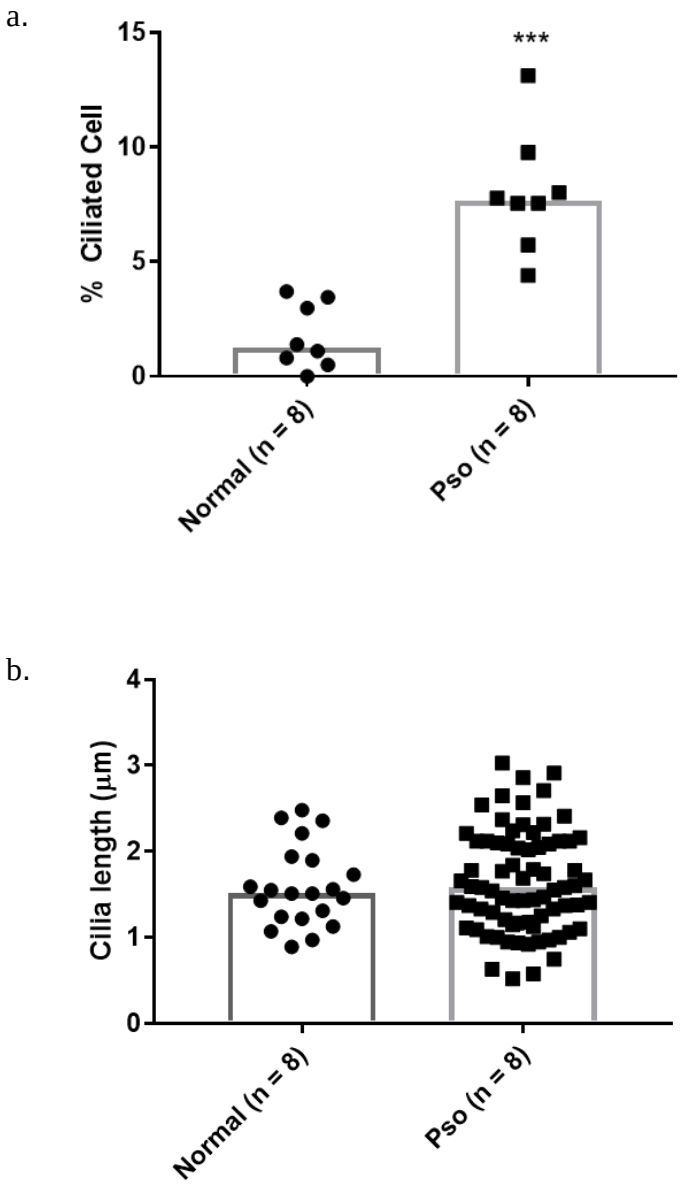

Figure 10

(a) Statistical analysis of ciliated cell percentage calculation in normal and psoriasis skin. About 500–700 cells from several locations of epidermal area were observed using confocal imaging. The number of primary cilia and cells in each picture were counted using ImageJ. Bar graph shows median. *** $P < 0.005$ (Mann Whitney U-Test). (b) Length of primary cilia both in normal and psoriasis skin. Approximately 500–700 cells from several locations of epidermal area were observed using confocal imaging, lengths of observed cilia were measured using ImageJ software.

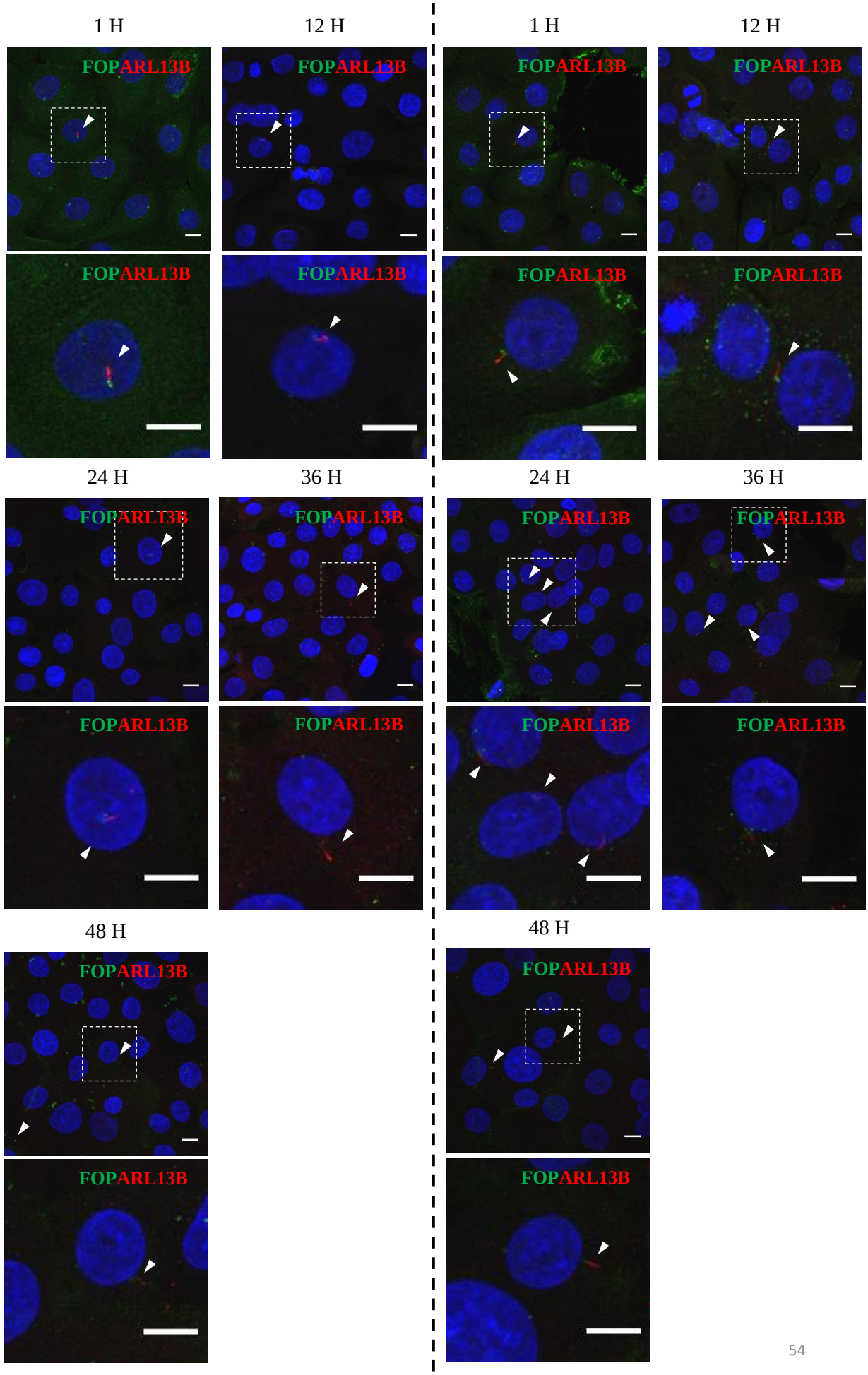
a. Normal Serum
b. Serum Starvation
1 H
12 H
1 H
12 H
FOPARL13B
24 H
36 H
24 H
36 H
48 H
48 H

Figure 11

12 Hours time point analysis of ciliogenesis in primary keratinocyte. Cells were grown in (a) normal serum and (b) serum starvation condition. NHEK were stained using anti-FOP (Green) and anti-ARL13B (red). Images were taken with a confocal microscope and were used to count the number of ciliated cells. The head arrow shows the primary cilia. Box indicates the enlarged area shown in the upper part of each picture. Scale bar = 10 μm.

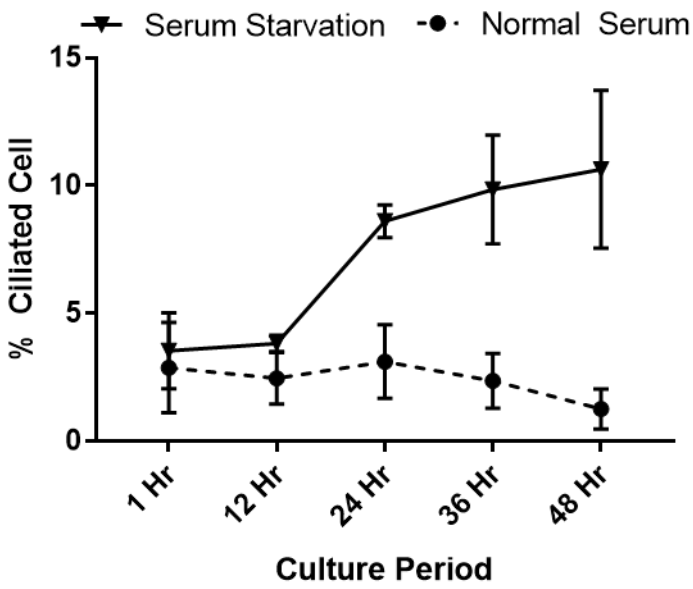

Figure 12
The ciliated cell percentage calculation in NHEK in 12 hours time point (for total 2 days experiment). Images from previous figure (Fig. 13) were used to count the number of ciliated cells..

a.

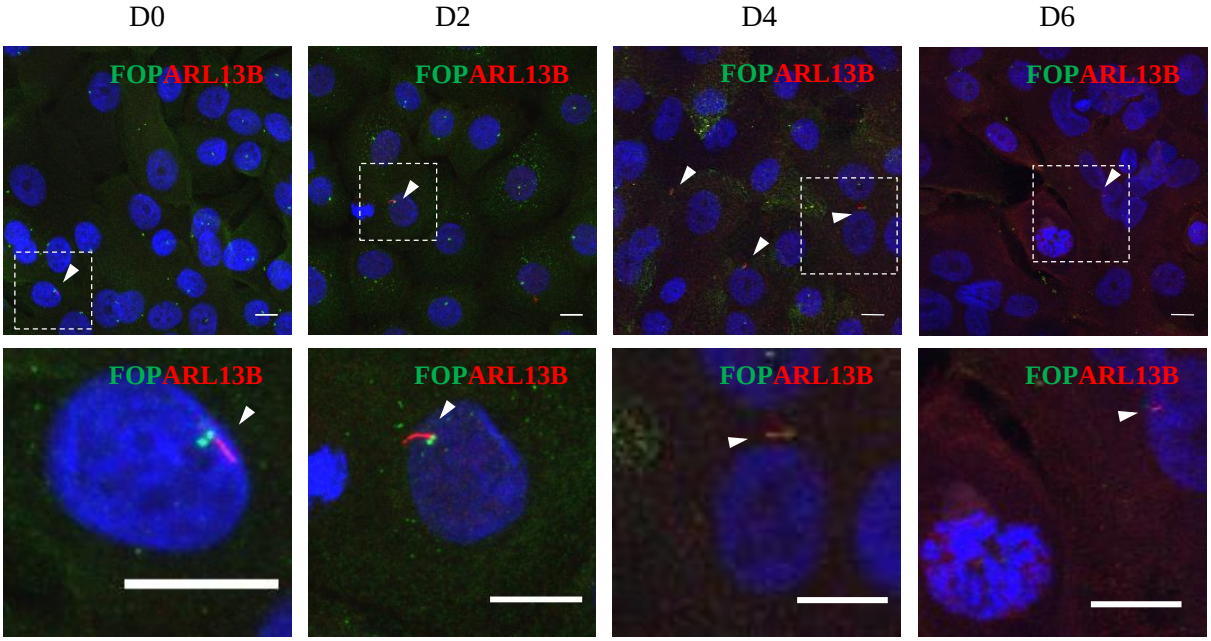

b.

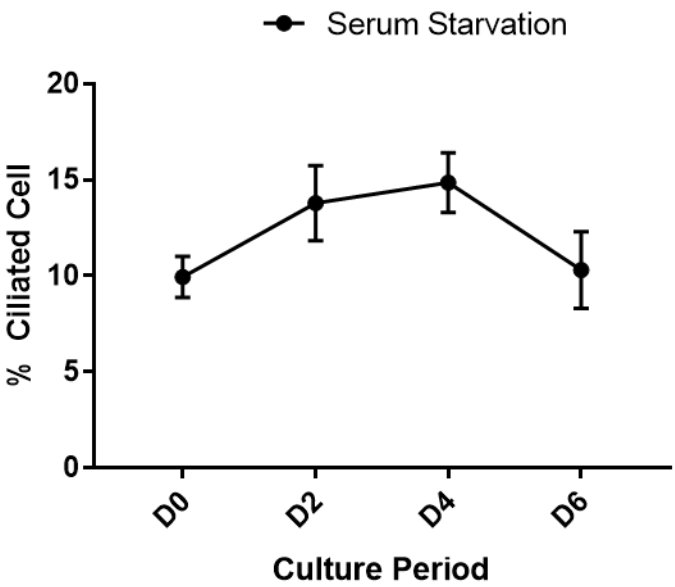

Figure 13
(a) 2 days time point analysis of ciliogenesis in primary keratinocyte. Cells were grown in serum starvation condition. NHEK were stained using anti-FOP (Green) and anti-ARL13B (red). Images were taken with a confocal microscope and were used to count the number of ciliated cells. The head arrow shows the primary cilia. Box indicates the enlarged area shown in the upper part of each picture. Scale bar = 10 µm. (b) The percentage of ciliated cell in serum starvation condition in 2 days (for total 6 days experiment).

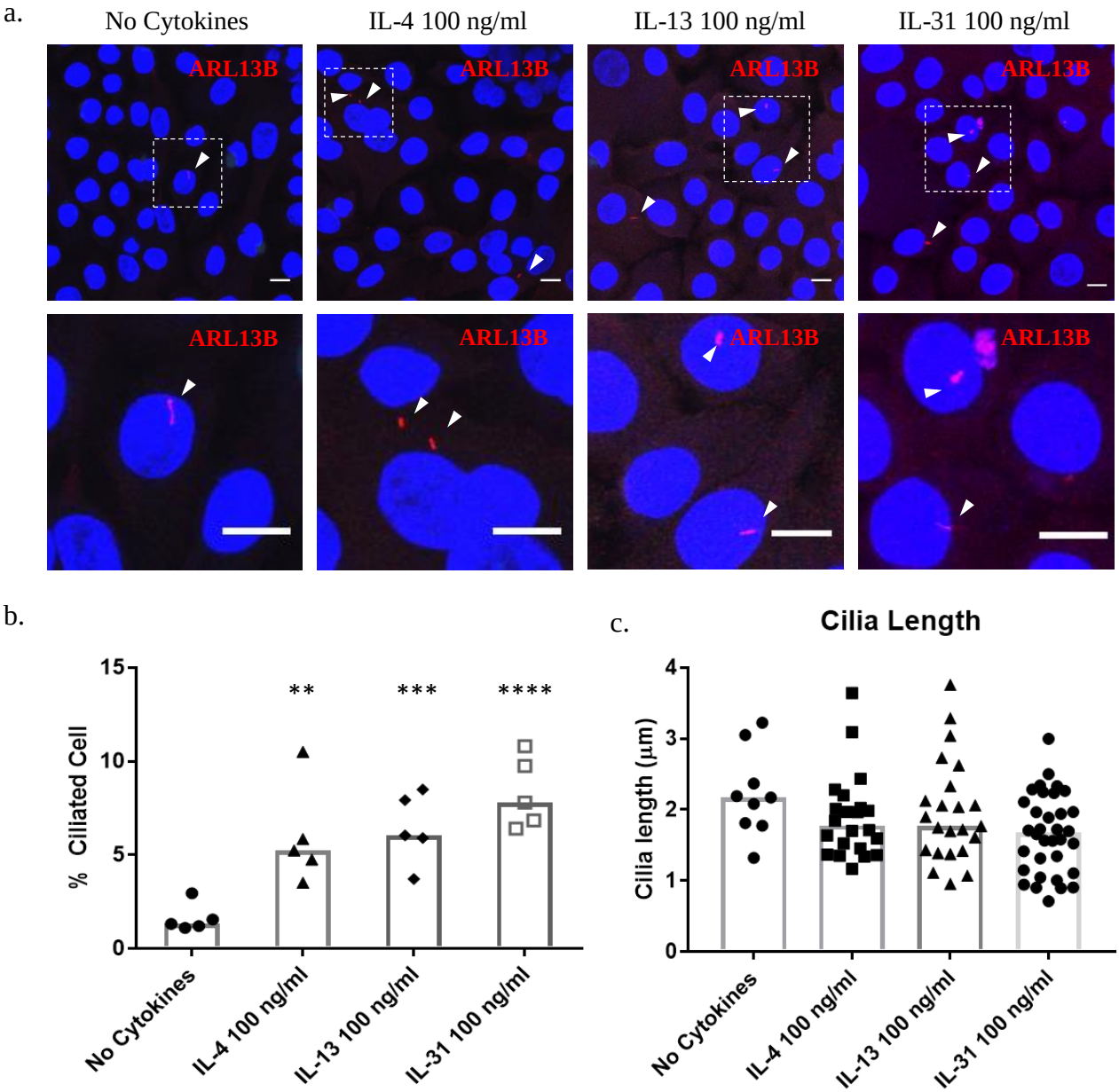

Figure 14

(a) After 48–hour stimulation with Th2 cytokines (IL-4, IL-13, and IL-31), NHEK were stained using anti-ARL13B (red). Images were taken with a confocal microscope and were used to count the number of ciliated cells. The head arrow shows the primary cilia. Box indicates the enlarged area shown in the upper part of each picture. Scale bar = 10 µm.

(b) The percentage of ciliated cells after NHEK stimulation using IL-4, IL-13, or IL-31. About 200–300 cells from several points on the culture slide were observed using confocal imaging. The number of primary cilia and cells in each picture counted using ImageJ software. Bar graph shows median. * $P < 0.05$, ** $P < 0.005$, **** $P < 0.0001$ (Bonferonni's test). (c) Cilia length in primary keratinocyte was measured using ImageJ after NHEK stimulation using IL-4, IL-13, and IL-31 cytokines. No significant difference was found compared to control.

a.

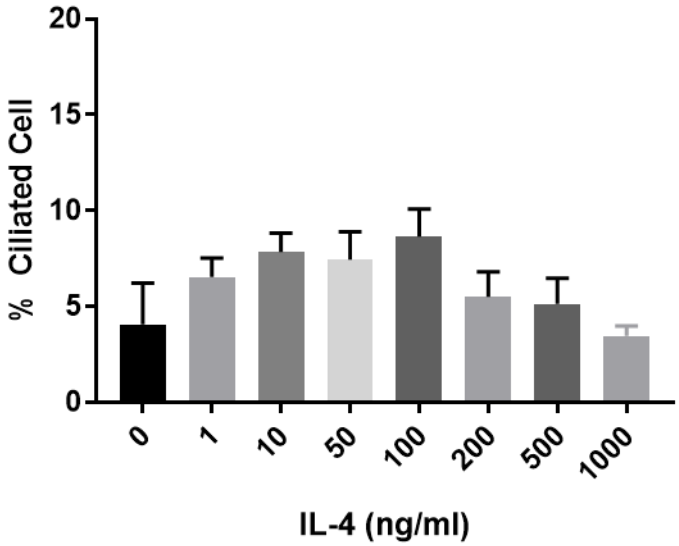

b.

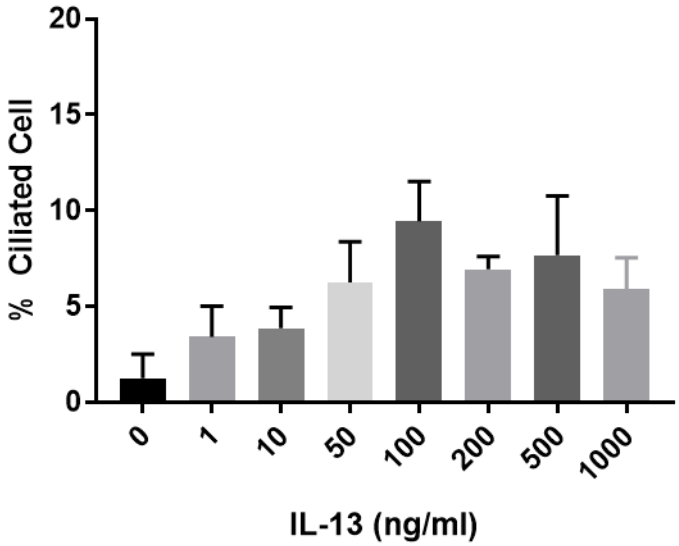

c.

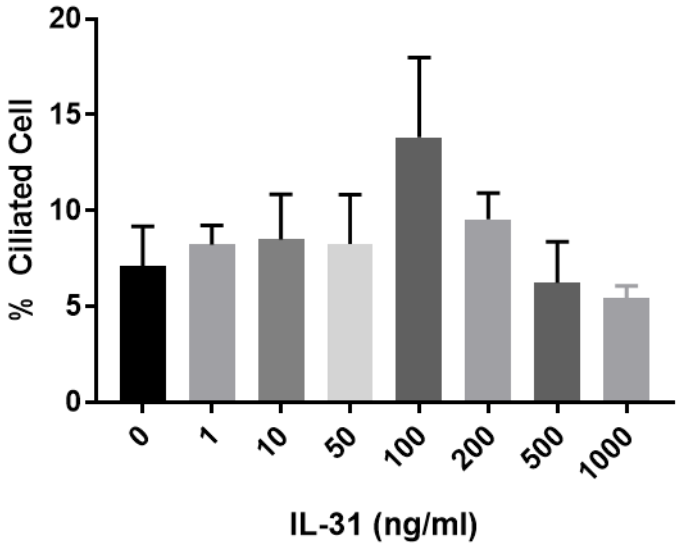

Figure 15

The ciliated cell percentage calculation in NHEK stimulated with Th2 cytokines in various concentration. About 200–300 cells from several points on the culture slide were observed using confocal imaging. The number of primary cilia and cells in each picture were counted using ImageJ. The cells were stimulated using (a) IL-4, (b) IL-13, (c) IL-31.

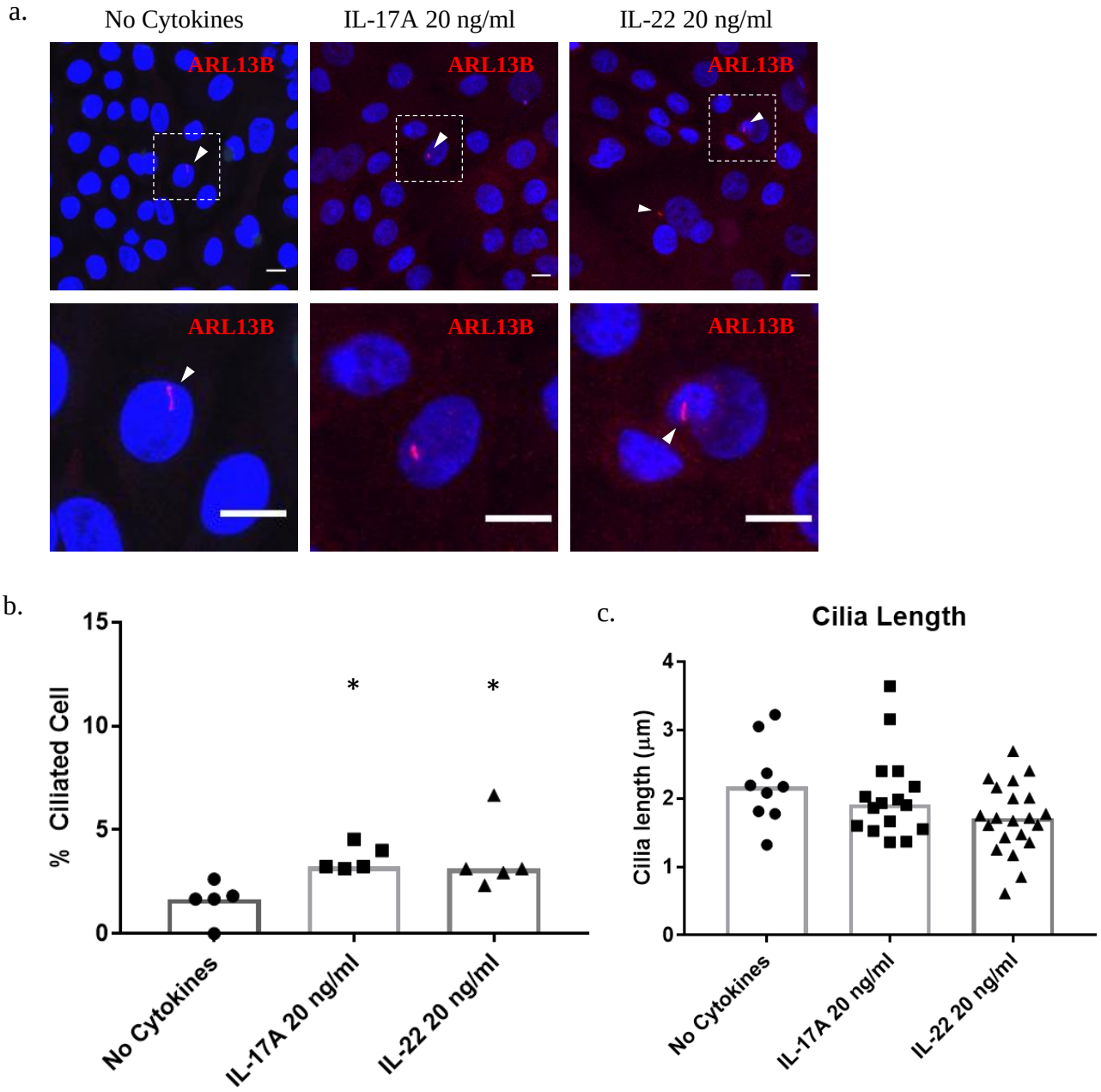

Figure 16

(a) After 48–hour stimulation with Th17 cytokines (IL-17A and IL-22), NHEK were stained using anti-ARL13B (red). Images were taken with a confocal microscope and were used to count the number of ciliated cells. The head arrow shows the primary cilia. Box indicates the enlarged area shown in the upper part of each picture. Scale bar = 10 µm.

(b) The percentage of ciliated cells after NHEK stimulation using IL-17A or IL-22. About 200–300 cells from several points on the culture slide were observed using confocal imaging. The number of primary cilia and cells in each picture counted using ImageJ software. Bar graph shows median. * $P < 0.05$ (Bonferonni's test). (c) Cilia length in primary keratinocyte was measured using ImageJ after NHEK stimulation using IL-17A and IL-22 cytokines. No significant difference was found compared to control.

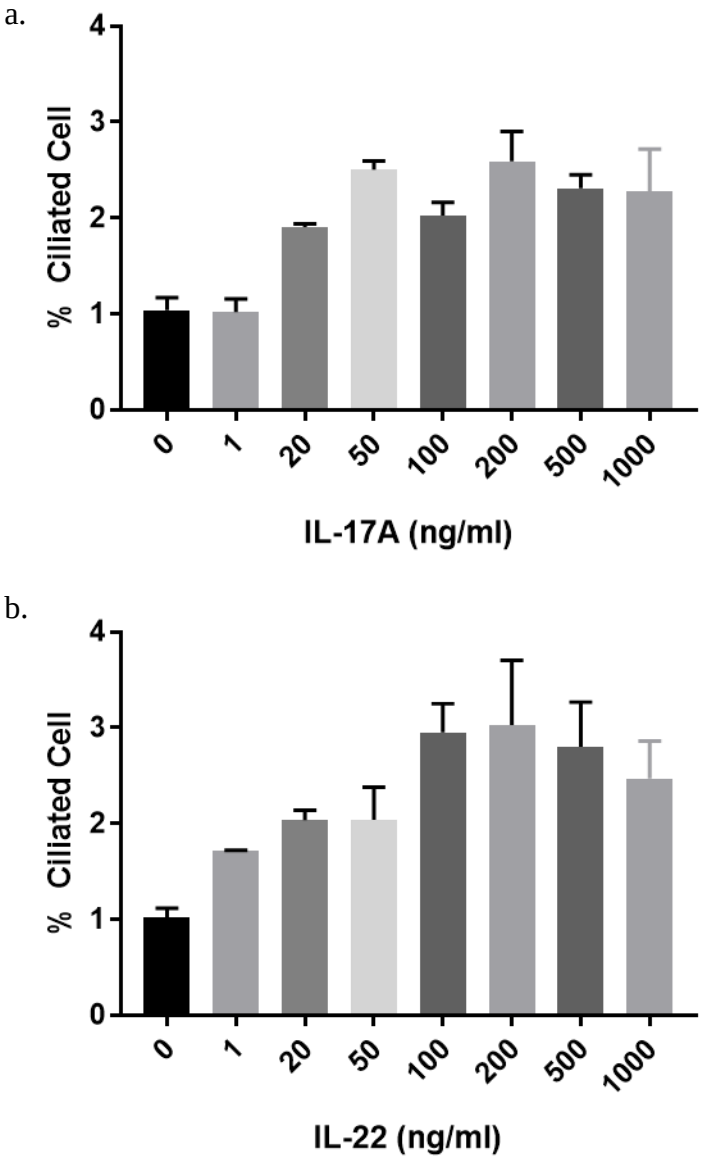

Figure 17
The ciliated cell percentage calculation in NHEK stimulated with Th17 cytokines in various concentration. About 200–300 cells from several points on the culture slide were observed using confocal imaging. The number of primary cilia and cells in each picture were counted using ImageJ. The cells were stimulated using (a) IL-17A (b) IL-22.

a.

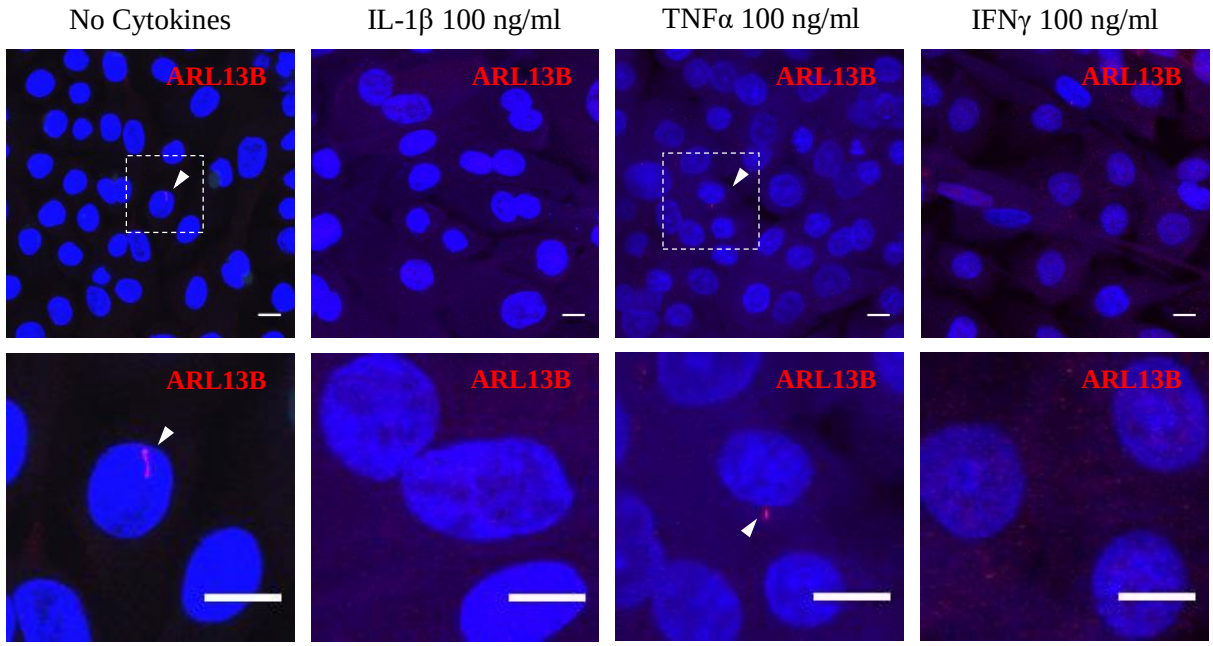

b.

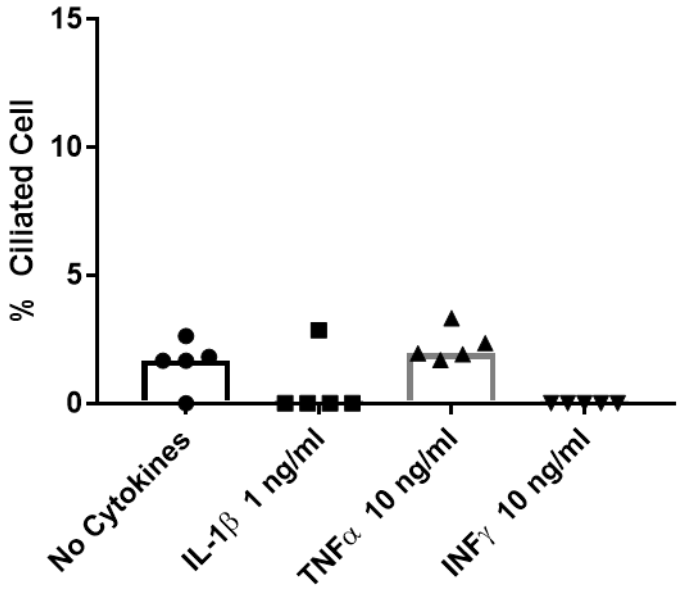

Figure 18

(a) After 48–hour stimulation with Th1 cytokines (IL-1β, TNFα, and IFNγ), NHEK were stained using anti-ARL13B (red). Images were taken with a confocal microscope and were used to count the number of ciliated cells. The head arrow shows the primary cilia. Box indicates the enlarged area shown in the upper part of each picture. Scale bar = 10 μm.

(b) The percentage of ciliated cells after NHEK stimulation using IL-1β, TNFα, or IFNγ. About 200–300 cells from several points on the culture slide were observed using confocal imaging. The number of primary cilia and cells in each picture counted using ImageJ software.

a.

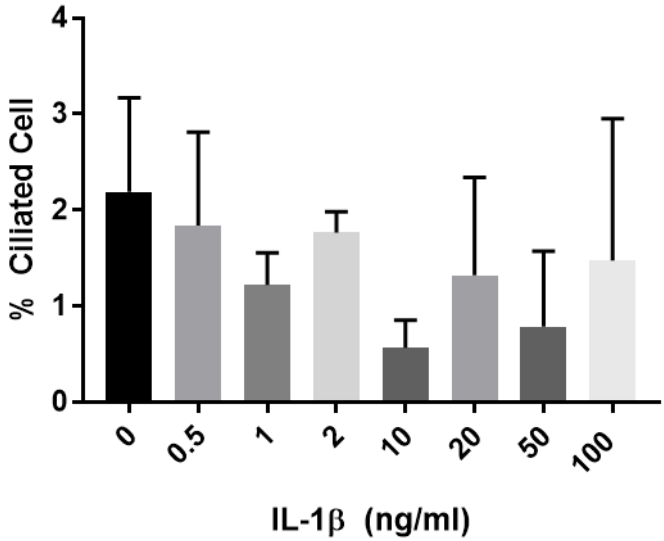

b.

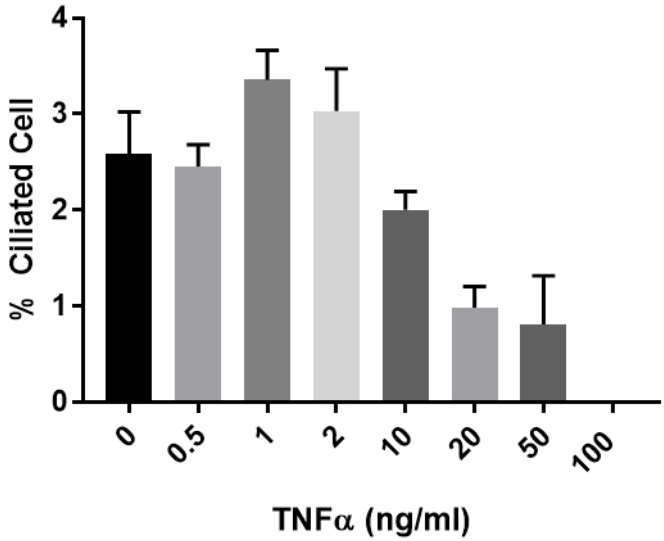

c.

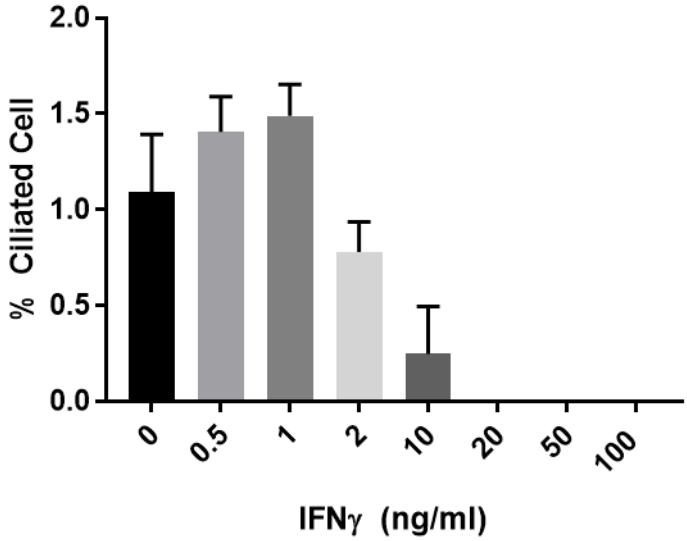

Figure 19

The ciliated cell percentage calculation in NHEK stimulated with Th1 cytokines in various concentration. About 200–300 cells from several points on the culture slide were observed using confocal imaging. The number of primary cilia and cells in each picture were counted using ImageJ. The cells were stimulated using (a) IL-1β (b) TNFα, (c) IFNγ.

a.

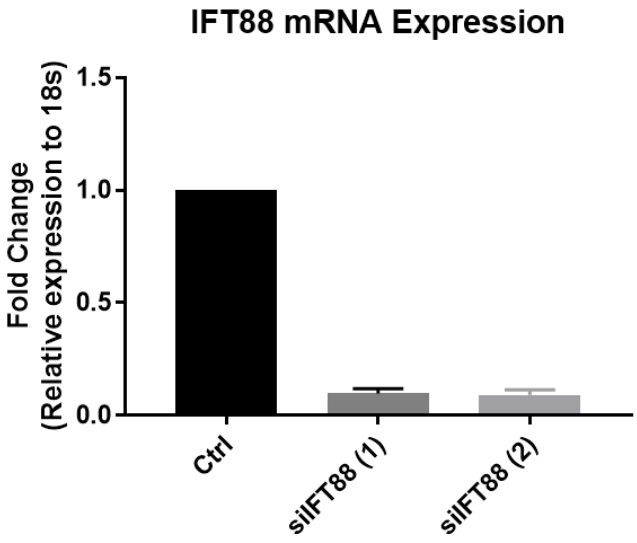

b.

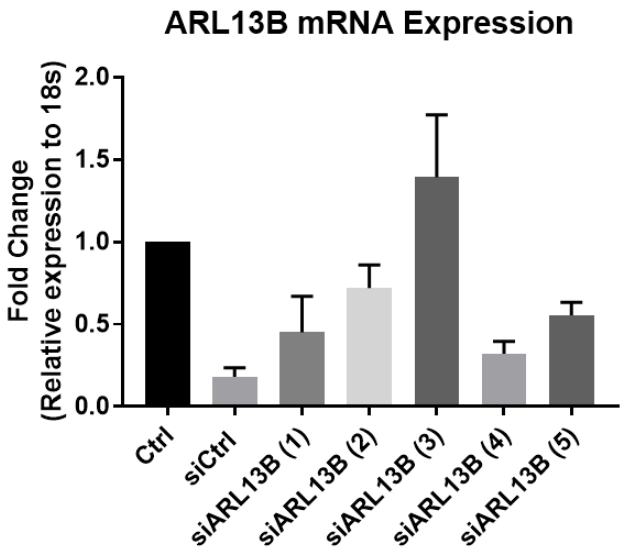

c.

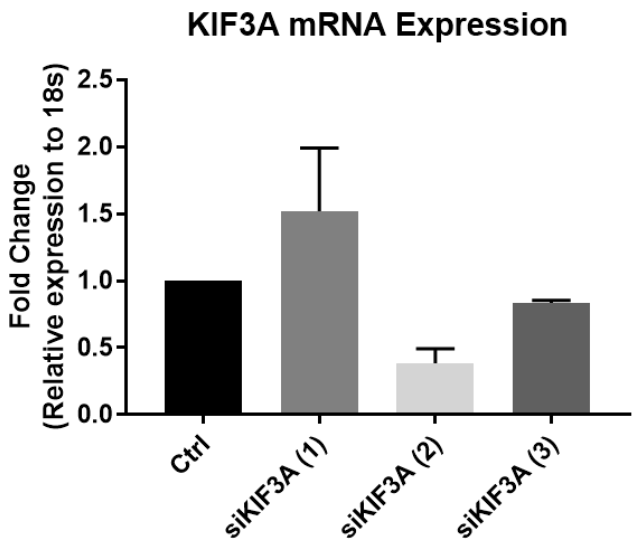

Figure 20
mRNA expression of multiple ciliary protein after siRNA knockdown experiment. Decrease of mRNA expression observed in several siRNA subtype (not all type in the siRNA set). mRNA expression in siRNA knockdown of (a) IFT88, (b) ARL13B, and (c) KIF3A.

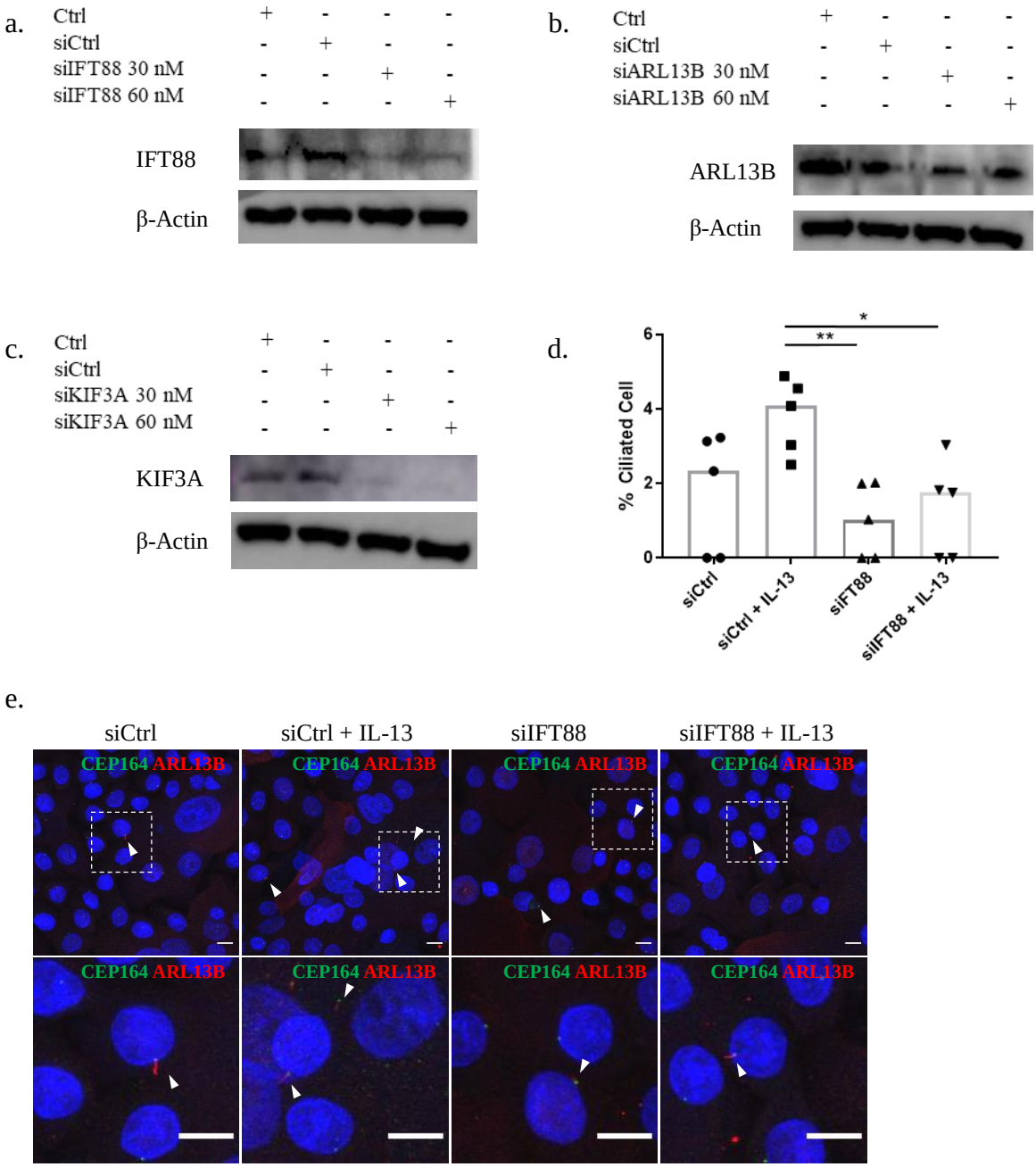

Figure 21
Ciliary Protein expression after siRNA knockdown experiment. Decrease of protein expression (compared either with Ctrl or siCtrl) observed in several siRNA knockdown of (a) IFT88, (b) ARL13B, and (c) KIF3A. (d) and (e) Immunostaining shows a decrease in the ciliated cell numbers after IFT88 expression was knocked down using siRNA in NHEK. * $P < 0.05$, ** $P < 0.005$ (Bonferonni's test). Images were captured with a confocal microscope, and were used to count the number of ciliated cells. The head arrow shows the primary cilia. Box indicates the enlarged area shown in the upper part of each picture. Scale bar = 10 µm

a.

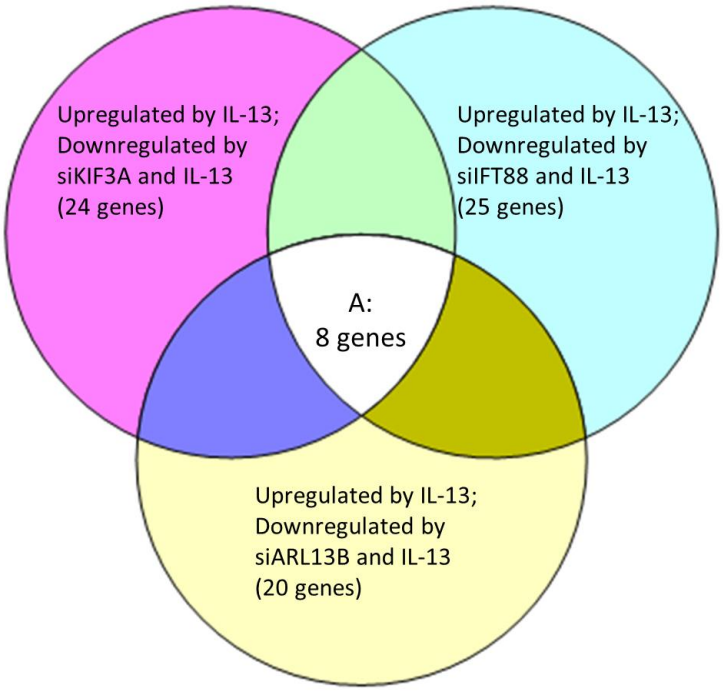

b.

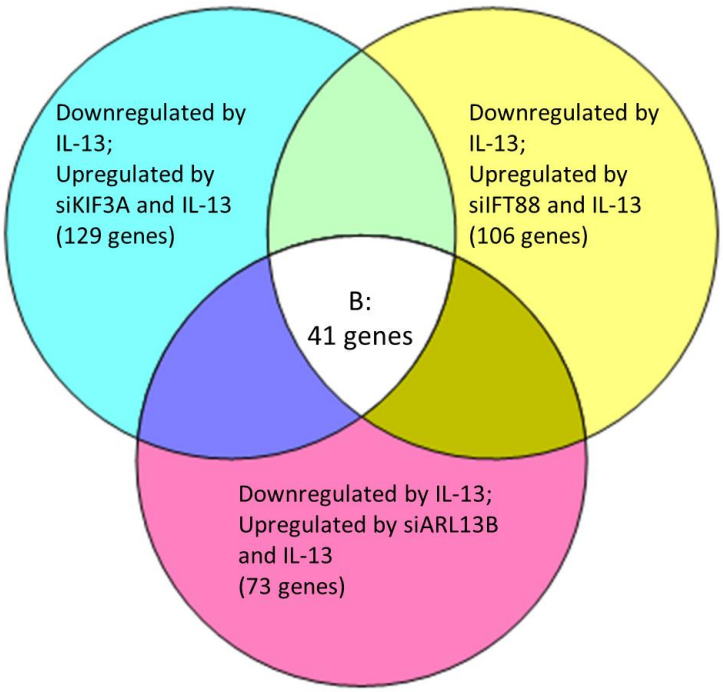

Figure 22
Venn diagram showed differential expressed genes which are detected by microarray. Total of 49 genes (a) Upregulated; 8 genes and (b) Downregulated; 41 genes, were affected after downregulation of primary cilia related genes (ARL13B, IFT88, or KIF3A) under stimulation of IL-13 (fold change were compared to Ctrl and siCtrl).

a.

siCtrl	+	+	+	+	-	-	-	-
siIFT88	-	-	-	-	+	+	+	+
IL-13 50 ng/ml	-	+	-	-	-	+	-	-
IL-17A 50 ng/ml	-	-	+	-	-	-	+	-
IL-22 50 ng/ml	-	-	-	+	-	-	-	+

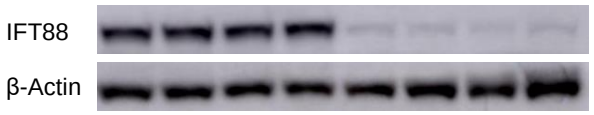

b.

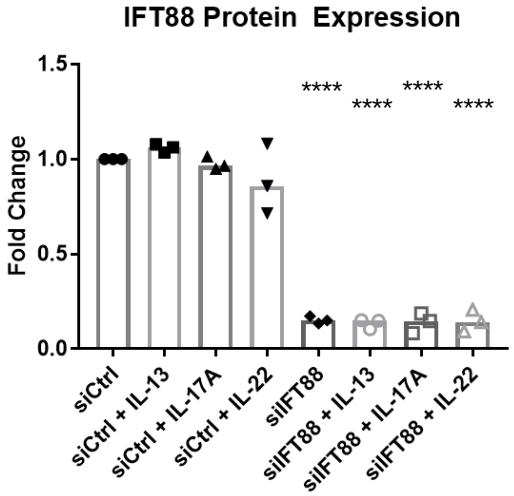

c.

siCtrl	+	+	+	+	-	-	-	-
siIFT88	-	-	-	-	+	+	+	+
IL-13 50 ng/ml	-	+	-	-	-	+	-	-
IL-17A 50 ng/ml	-	-	+	-	-	-	+	-
IL-22 50 ng/ml	-	-	-	+	-	-	-	+

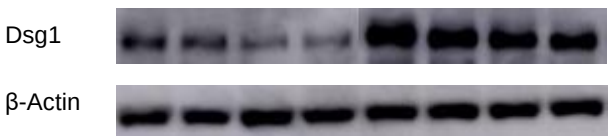

d.

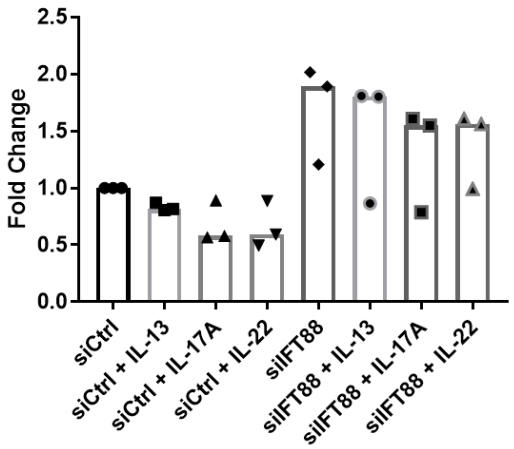

Figure 23

(a) and (b) Western blot results showing the significant downregulation of IFT88 protein after siRNA knockdown, also in IL-13, IL-17a and IL-22 stimulation, as statistically analyzed by Bonferonni's test (**** $P < 0.0001$). Fold change based on siCtrl value. (c) and (d) Th2 and Th17 cytokines stimulation on NHEK caused the downregulation of Dsg1. IFT88 knockdown upregulated Dsg1 expression. Fold change based on siCtrl value.

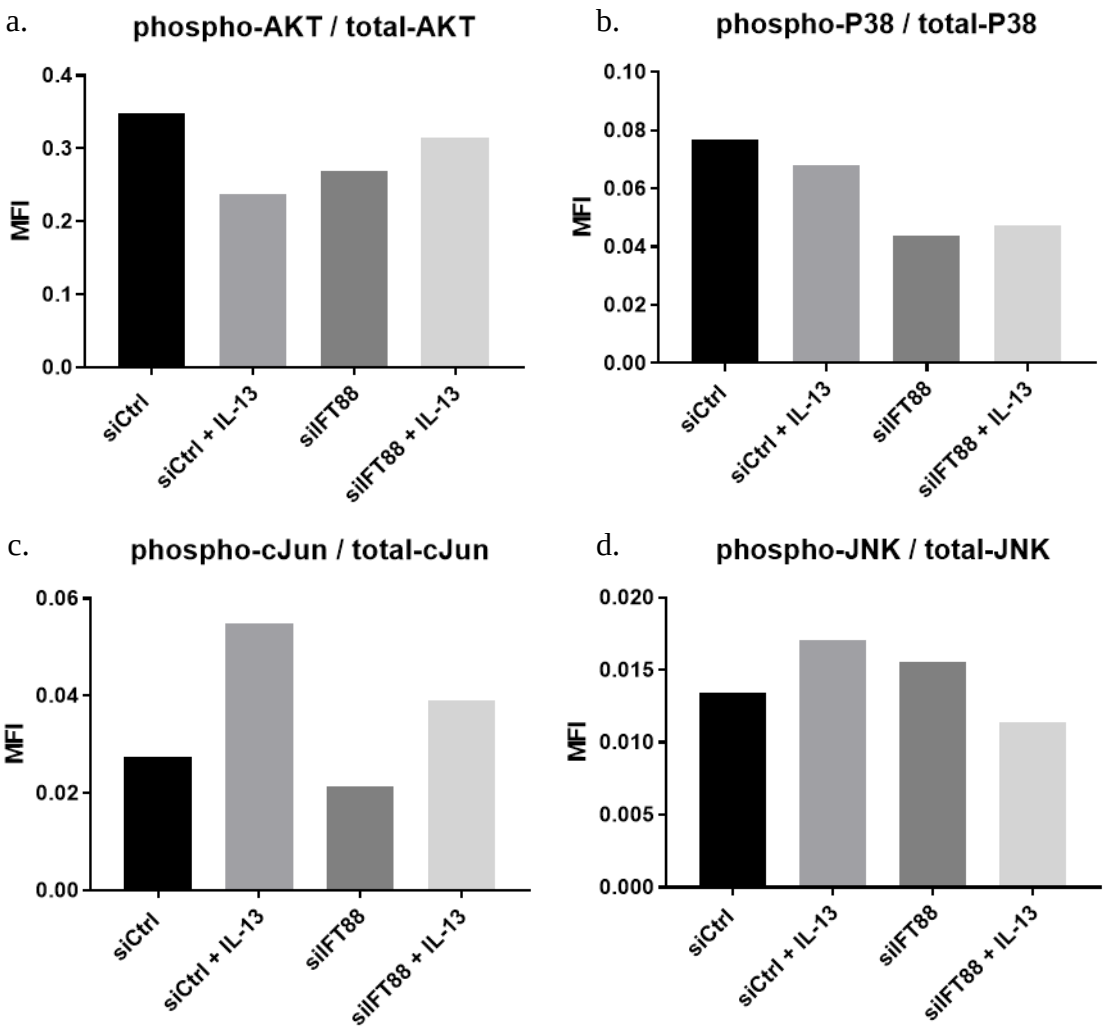

Figure 24
IL-13 stimulation and IFT88 knockdown on PK caused various responses on the phosphorylation of several signaling molecule (a) AKT, (b) P38, (c) c-JUN, and (d) JNK.

a.

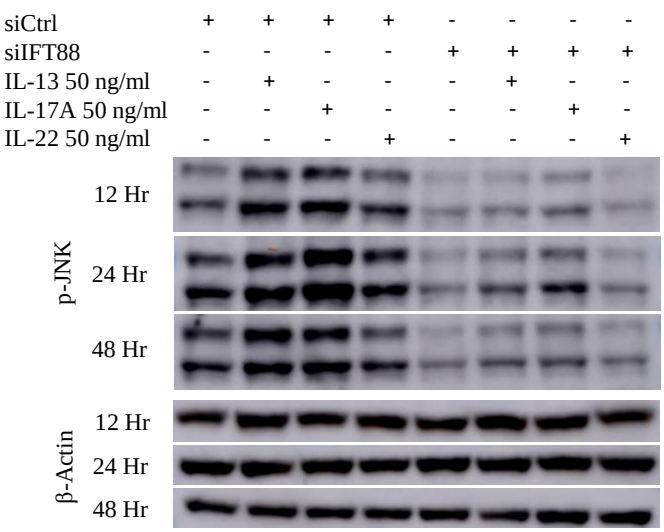

b.

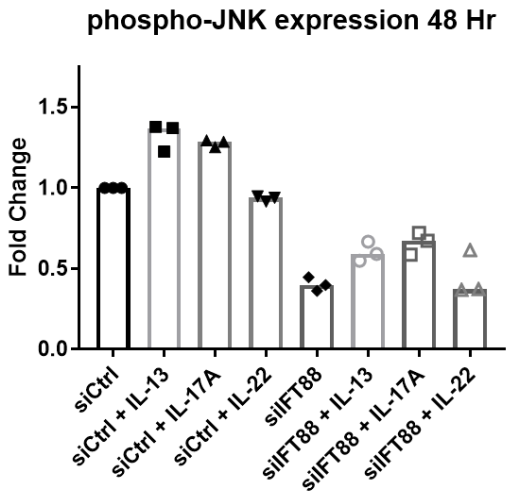

Figure 25
(a) and (b) Western blot analysis show the downregulation of JNK phosphorylation was found as consequence of IFT88 knockdown.

a.

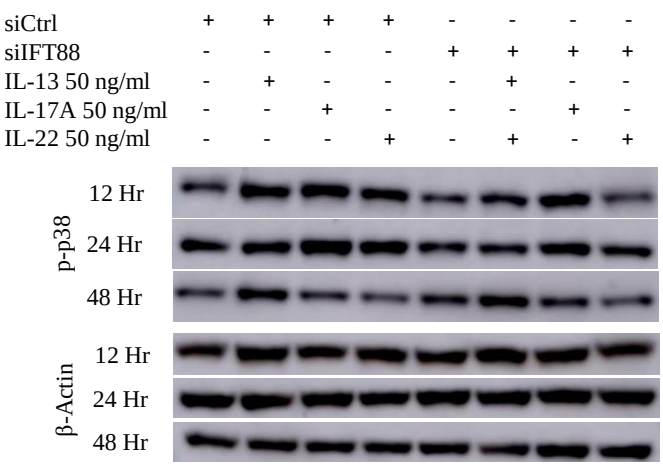

b.

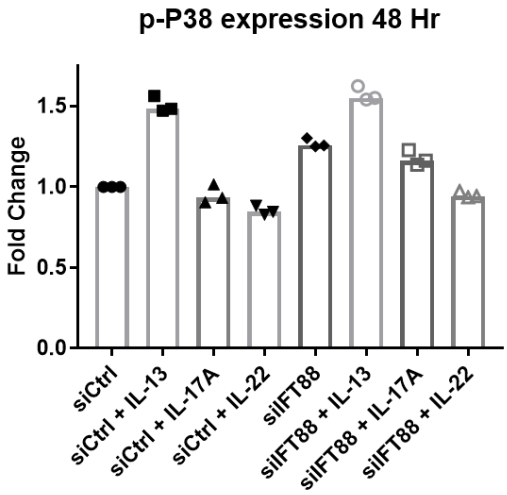

Figure 26
(a) and (b) Western blot analysis show the expression of P38 phosphorylation which was not affected as much as JNK phosphorylation after IFT88 knockdown.

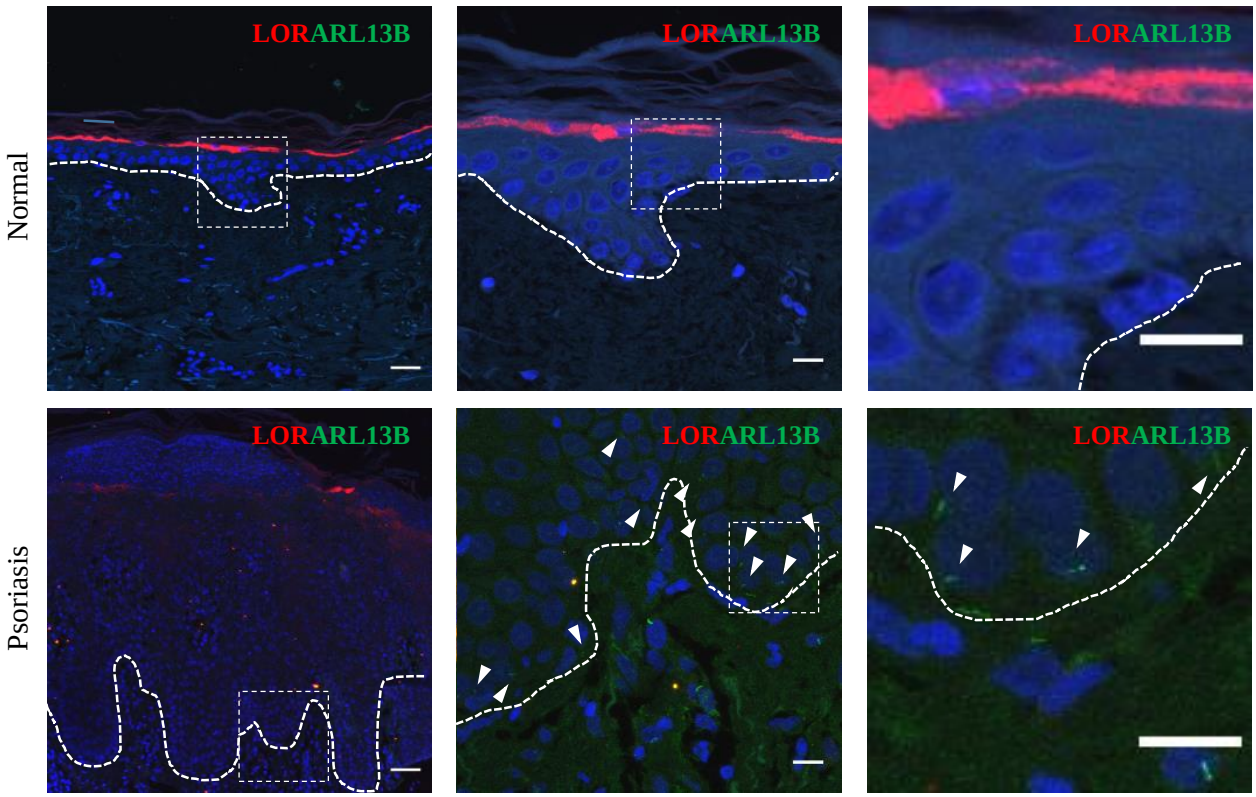

Figure 27

Fluorescent IHC image of normal and psoriasis skin, stained using anti-loricrin (Red) and anti-ARL13B (Green). White dash shows the basal line, upper part of the dash indicates the epidermis whereas dermis area located below the dash. The box indicated the enlarged area shown in the picture on the left side of each picture. Arrowheads show primary cilia. Scale bar 25 µm (normal skin, left panel) 50 µm (psoriasis skin, left panel), 10 µm (middle and right panel).

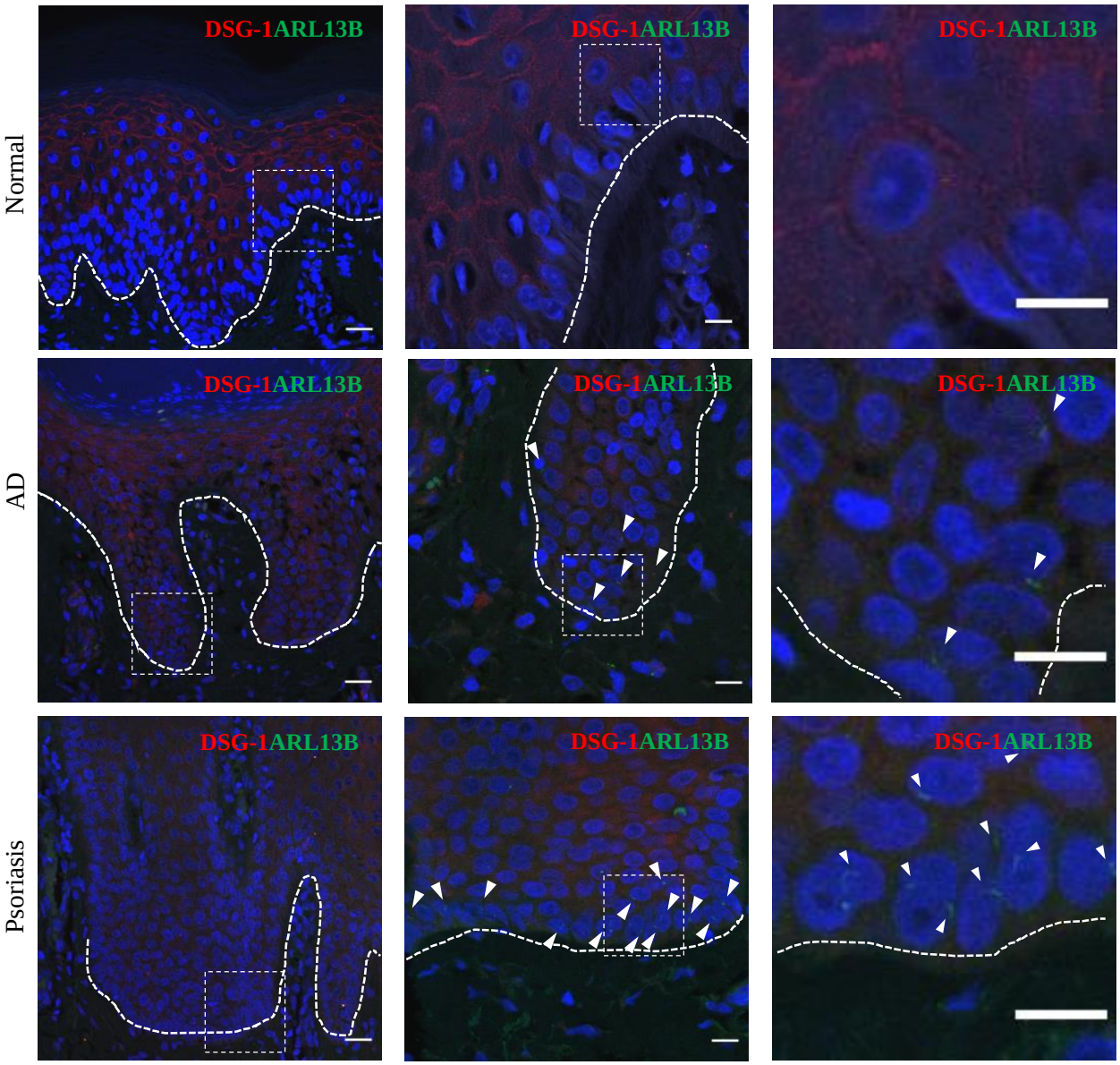

Figure 28

Fluorescent IHC image of normal, AD, and psoriasis skin, stained using anti-desmoglein 1 (Red) and ARL13B (Green). White dash shows the basal line, upper part of the dash indicates the epidermis whereas dermis area located below the dash. The box indicated the enlarged area shown in the picture on the left side of each picture. Arrowheads show primary cilia. Scale bar 50 µm (left panel), 10 µm (middle and right panel).

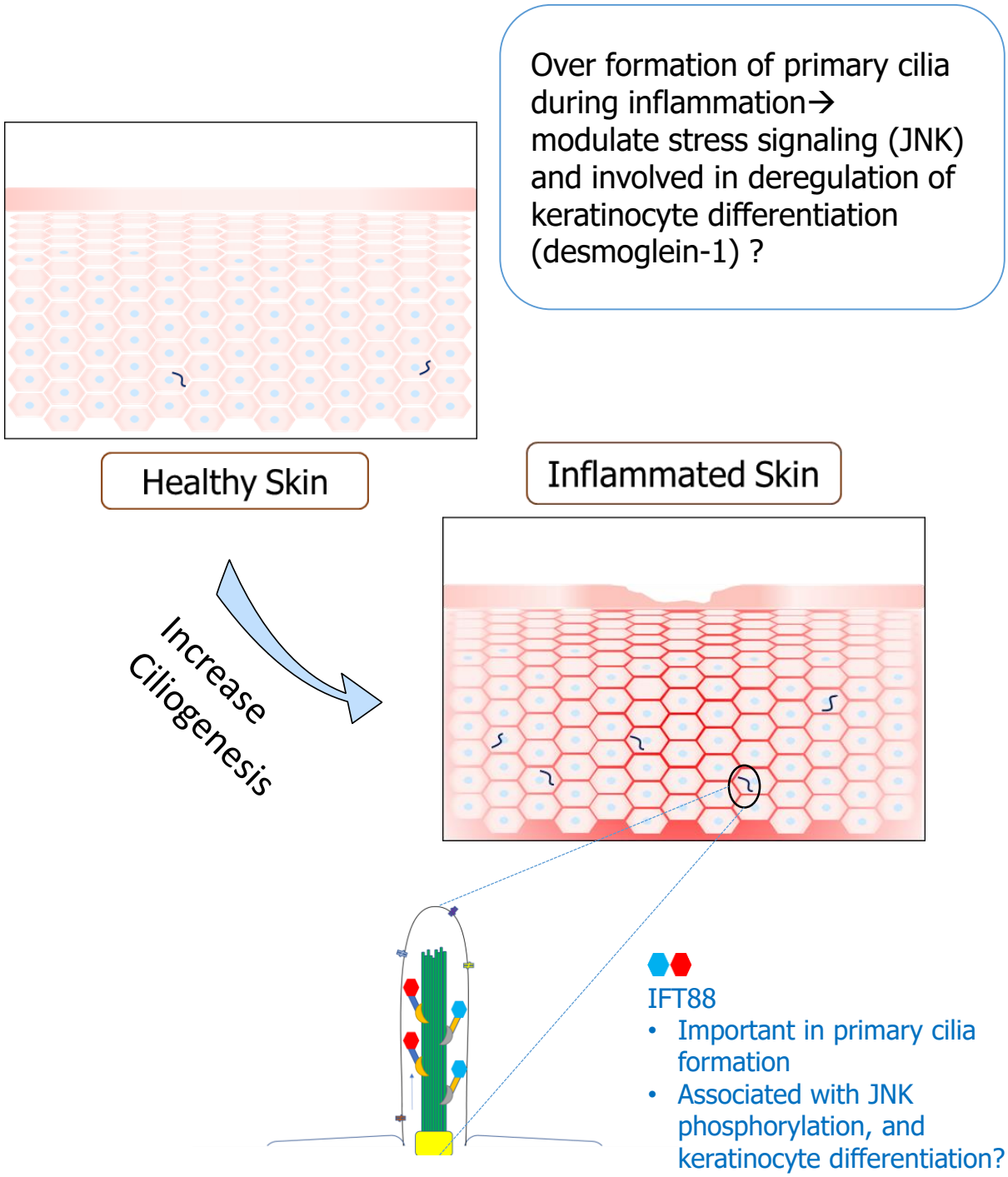

Figure 29
Possible schematic mechanism ruled by primary cilia in akin inflammation (atopic dermatitis and psoriasis). As IFT88, ciliogenesis protein, show association with JNK phosphorylation and modulate desmoglein-1, primary cilia have important role in the progression of skin inflammation.

Table 1.
List of antibody product used in immunohistochemistry (IHC) and immunocytochemistry (ICC) experiment.

Purpose	Primary Antibody	Company	Catalog Number	Dilution
IHC	Anti-Acetylated α tubulin	Millipore Sigma	T7451	1:1000
IHC	Anti-Pericentrin	Abcam	ab220784	1:2000
IHC	Anti-ARL13B	Abcam	ab136648	1:500
IHC	Anti-Cytokeratin 14 (K14)	Abcam	ab7800	1:100
IHC	Anti-Cytokeratin 15 (K15)	Abcam	ab52816	1:100
IHC	Anti-Loricrin	Abcam	ab176322	1:250
IHC	Anti-Desmoglein 1	Abcam	ab124798	1:250
ICC	Anti-FOP	Abnova	H00011116-M01	1:1000
ICC	Anti-CEP164	Santa Cruz Biotechnology	sc-515403	1:250
ICC	Anti-ARL13B	Proteintech	17711-1-AP	1:1000

Table 2.
List of siRNA sequence used in the RNA interference experiment.

siRNA	Sense	Anti Sense
IFT88(1)	CCAAGUGUCAAUAAGCAAAtt	UUUGCUUAUUGACACUUGGaa
IFT88(2)	GGUAGCUAGUUGUUUCAGAtt	UCUGAAACAACUAGCUACCat
ARL13B(1)	GAACGCAUCCAAAAAGAGAtt	UCUCUUUUUGGAUGCGUUCat
ARL13B(2)	GCAGUUAAAGAAUGAAGAUtt	AUCUUCAUUCUUUAACUGCtg
ARL13B(3)	GAGCUGAACGAGUGCGAAAtt	UUUCGCACUCGUUCAGCUCtt
ARL13B(4)	GGACUAGUAGAAAAUUAUAtt	UAUAAUUUUCUACUAGUCCaa
ARL13B(5)	CAGCUAAUGGUAAAAAGAAtt	UUCUUUUUACCAUUAGCUGat
KIF3A(1)	GCAUUGAUGGUAAGAUGCAtt	UGCAUGUUACCAUCAAUGCct
KIF3A(2)	GCAUAUGGACAAACCGGAAtt	UUCCGGUUUGUCCAUUAGCaa
KIF3A(3)	CUAUCAGUACAUUACGGUAtt	UACCGUAAUGUACUGAUAGtt

Table 3.
List of primer sequence used in the qRT-PCR experiment.

Primer	Forward	Reverse
IFT88	TCGGCTAGATGAGGCTTTGGAC	CACTGACCACCTGCATTAGCCA
ARL13B	GAACCAGTGGTCTGGCTGAGTT	GTTTCAGGTGGCAGCCATCACT
KIF3A	CTGATATCAGTGGGTCAGAGGA	TCCAGCAAAGACTGATGCTCT
18S	CGGCTACCACATCCAAGGAA	AGCTGGAATTTTACCCGCGGC

Table 4.
List of affected (a) Upregulated and (b) Downregulated genes which show correlation with ARL13B, IFT88, or KIF3A knockdown; and IL-13 stimulation in primary keratinocyte.

a.

ID	Gene Symbol	Description
203439_s_at	STC2	stanniocalcin 2
204126_s_at	CDC45	cell division cycle 45
204463_s_at	EDNRA	endothelin receptor type A
204464_s_at	EDNRA	endothelin receptor type A
210809_s_at	POSTN	periostin, osteoblast specific factor
216235_s_at	EDNRA	endothelin receptor type A
220892_s_at	PSAT1	phosphoserine aminotransferase 1
1555778_a_at	POSTN	periostin, osteoblast specific factor

b.

ID	Gene Symbol	Description
203845_at	KAT2B	K(lysine) acetyltransferase 2B
209373_at	MALL	mal, T-cell differentiation protein-like
1558105_a_at	SLC9A7	solute carrier family 9, subfamily A (NHE7, cation proton antiporter 7), member 7
206193_s_at	CDSN	corneodesmosin
220620_at	CRCT1	cysteine rich C-terminal 1
206884_s_at	SCEL	sciellin
232056_at	SCEL	sciellin
1554921_a_at	SCEL	sciellin
205730_s_at	ABLIM3	actin binding LIM protein family, member 3
1564307_a_at	A2ML1	alpha-2-macroglobulin-like 1
222242_s_at	KLK5	kallikrein related peptidase 5
212531_at	LCN2	lipocalin 2
205680_at	MMP10	matrix metallopeptidase 10
231579_s_at	TIMP2	TIMP metallopeptidase inhibitor 2
209792_s_at	KLK10	kallikrein related peptidase 10
203757_s_at	CEACAM6	carcinoembryonic antigen-related cell adhesion molecule 6 (non-specific cross reacting antigen)
211657_at	CEACAM6	carcinoembryonic antigen-related cell adhesion molecule 6 (non-specific cross reacting antigen)
243463_s_at	RIT1	Ras-like without CAAX 1
213927_at	MAP3K9	mitogen-activated protein kinase kinase kinase 9
202935_s_at	SOX9	SRY box 9
236313_at	CDKN2B	cyclin-dependent kinase inhibitor 2B (p15, inhibits CDK4)
203571_s_at	ADIRF	adipogenesis regulatory factor
204734_at	KRT15	keratin 15, type I
238550_at	RUFY2	RUN and FYVE domain containing 2
230760_at	ZFY	zinc finger protein, Y-linked
235165_at	PARD6B	par-6 family cell polarity regulator beta
215501_s_at	DUSP10	dual specificity phosphatase 10
221563_at	DUSP10	dual specificity phosphatase 10
229114_at	GAB1	GRB2-associated binding protein 1
226158_at	KLHL24	kelch-like family member 24
203453_at	SCNN1A	sodium channel, non voltage gated 1 alpha subunit
206642_at	DSG1	desmoglein 1
1552797_s_at	PROM2	prominin 2
237690_at	ADGRF4	adhesion G protein-coupled receptor F4
201428_at	CLDN4	claudin 4
219795_at	SLC6A14	solute carrier family 6 (amino acid transporter), member 14
226189_at	ITGB8	integrin beta 8
228221_at	SLC44A3	solute carrier family 44, member 3
210065_s_at	UPK1B	uroplakin 1B
219756_s_at	POF1B	premature ovarian failure, 1B
227272_at	C15orf52	chromosome 15 open reading frame 52